

Lidar-Based Models of Understory Bird Habitat in a Tropical Forest

by

Amanda G. Grimm

A thesis submitted in partial fulfillment of
the requirements for the degree of
Master of Science
Conservation Biology

School of Natural Resources and Environment
University of Michigan, Ann Arbor
December 2011

Thesis committee:
Dr. Kathleen Bergen
Dr. Leland Pierce

Table of Contents

List of Figures	ii
List of Tables	ii
1 ABSTRACT.....	1
2 INTRODUCTION	1
2.1 Goal and Objectives	3
3 STUDY SITE.....	3
4 DATA AND METHODS	4
4.1 Field Data.....	5
4.1.1 Forest Field Data.....	5
4.1.2 Bird Data.....	6
4.2 Lidar and Other Spatial Data	7
4.2.1 LVIS Data and Creation of Lidar Metrics	7
4.2.2 Ancillary Spatial Data.....	9
4.3 Relating Lidar Metrics to Field Data	10
4.4 Bird Distribution Analysis	11
4.4.1 Modeling Diversity of Understory Insectivores	11
4.4.2 Models of Suitable Habitat	12
4.4.3 Model Testing	12
4.5 Fractal Tree Models	13
5 RESULTS	14
5.1 Lidar Metrics of Forest Structure.....	14
5.2 Bird Distribution Models	15
5.3 Fractal Tree Models	17
6 DISCUSSION	17
6.1 Lidar vs. Field Metrics	17
6.2 Maxent Models	18
6.3 Ability of lidar to measure forest understory	20
6.4 Implications for conservation of understory insectivores	21
6.5 Ongoing and future work.....	22

7 CONCLUSIONS.....	22
8 APPENDICES	23
8.1 Appendix 1: Mapped environmental variables used in MaxEnt models.....	23
8.2 Appendix 2: Growth forms and adult statures of La Selva tree species, used for parameterizing fractal models.....	56
8.3 Appendix 3: Species-specific wood densities used to estimate tree biomass.....	59
9 BIBLIOGRAPHY	63

List of Figures

Figure 1. Regional land use for the La Selva area and boundaries of the La Selva / Braulio Carrillo protected area and the study area of interest (AOI).....	4
Figure 2. Locations of forest inventory plots within the protected area.....	6
Figure 3. Field estimate of understory density vs. rh25.....	14
Figure 4. MaxEnt projections of distribution of potential habitat for four bird species of interest across the study area	16
Figure 5: Fractal model of TEAM vegetation plot 1.	17
Figure 6. Response of bird species to canopy cover.....	20

List of Tables

Table 1. Multi-dimensional habitat structure variables used in modeling.....	9
Table 2. Correlations between field and lidar-based estimates of understory structure.....	15
Table 3. Results of jackknife validations of MaxEnt models.....	16
Table 4. Environmental variables which contributed significantly to each species model	16

1 ABSTRACT

Where a poorly understood group of wildlife species seems to be declining quickly, a rapid assessment of the species' habitat requirements may be needed in order to make the most optimal management decisions possible. We used bird presence data and a combination of field data and full-waveform lidar data to predict and interpret the distributions of declining insectivorous understory bird species at the La Selva Biological Station in Costa Rica. Raw lidar waveforms were used to create metrics of multi-dimensional forest structure which take into account not only horizontal structure such as patches and their arrangement or fragmentation, but also the vertical structure of vegetation such as canopy height and the distribution of canopy layers. Habitat models for four species of understory insectivore were developed using MaxEnt and validated using a jackknife approach, while guild diversity was estimated across the landscape using multiple logistic regression. Habitat projections for individual species showed high and significant predictive ability in jackknife tests. Results of habitat modeling showed significant differences between species in terms of which habitat variables were most important, but percent cover, distance to forest edge, foliage height diversity, and canopy height were consistently important. Metrics derived from canopy height profiles were consistently more useful predictors than metrics from the raw lidar waveforms.

General metrics such as canopy height, elevation, and distance to edge were generally more useful predictors than understory-specific metrics, which could indicate that understory insectivores respond more strongly to climate & habitat patch size than to understory structure at a micro level. Alternatively, large-footprint lidar may be unable to adequately represent the aspects of understory structure which impact understory birds. Overall, however, models which included canopy height profile metrics significantly improved upon models which did not, indicating that inclusion of measures of multi-dimensional forest structure which account for the understory may add value to lidar-based habitat models for many wildlife species.

2 INTRODUCTION

Where a poorly understood group of wildlife species seems to be declining quickly, a rapid assessment of the species' habitat requirements may be needed in order to make the most optimal management decisions possible. In this type of situation, a habitat model based on characteristics which can be mapped across a landscape via remote sensing may be more useful than a model requiring collection of field data, which is generally both time and labor intensive.

Topography, microclimate, and forest community composition have long been recognized as important components of landscape-level models of forested habitat. More recently, characteristics of multi-dimensional forest structure have also emerged as important predictors of presence of wildlife species, habitat use, and species diversity. Multi-dimensional forest

structure takes into account not only horizontal structure such as patches and their arrangement or fragmentation, but also the vertical structure of vegetation such as canopy height and the distribution of canopy layers (Turner et al. 2003, Bergen 2006, Bergen et al. 2007, Goetz et al. 2007, Vierling et al. 2008). Multi-dimensional forest structure, particularly the vertical aspect, has been difficult to quantify and thus has received less attention as a determinant of habitat suitability. However, it clearly affects wildlife species both directly, by determining the arrangement of sites for nesting, foraging, resting, and mating, and indirectly, by impacting site microclimate and distribution of animal prey (Kapos 1989, Brokaw 1999, Pearman 2002). Important specific multi-dimensional characteristics of habitat include canopy height, presence of canopy layers, presence of an understory, canopy closure, vertical distribution of biomass, and size and frequency of gaps (MacArthur and MacArthur 1961, Schemske and Brokaw 1981, McShea and Rappole 2000, Hill et al. 2004).

The development of lidar remote sensing has recently made it possible to quantify attributes of multi-dimensional forest structure across relatively larger spatial extents and at higher spatial resolutions than were previously possible via field measurements and/or traditional remote sensing, respectively (Lefsky et al. 2002). Recent studies have used lidar data, on its own and in combination with ancillary data sources, to map attributes such as biomass, canopy height and cover, distribution of understory vegetation, and canopy height profiles (Drake et al. 2002a, Drake et al. 2002b, Martinuzzi et al. 2009). Thus, availability of lidar data and lidar-derived metrics presents opportunities to better understand how forested landscape multi-dimensional structure relates to habitat suitability for taxa where that information is lacking & difficult to obtain.

Many of the limits of lidar sensing of forest structure remain unclear, including the extent to which understory vegetation can be quantified (Martinuzzi et al. 2009). This is particularly true in dense, heterogeneous tropical forests, such as that of La Selva Biological Station in Costa Rica (Hofton et al. 2002, Lefsky et al. 2002). Mapping the understory structure at La Selva is of particular interest due to the rapid decline of understory bird populations at the site, particularly insectivorous species (Sigel et al. 2006). Declines in populations of understory insectivore (UI) species have been observed at many forested sites in the neotropics (Şekercioglu et al. 2002), with multiple proposed hypotheses for the decrease. Most explanations are related to habitat fragmentation as the root cause of the decline. Theories have included the UI guild's tendencies towards large home ranges, limited dispersal, and avoidance of forest edges. However, many of the UI species in decline at La Selva remain abundant at the nearby and much smaller (345 ha vs. 1600 ha) Tirimbina Rainforest Center (Roberts 2007). Another possibility is that the declines are being driven, either directly or indirectly, by changes in the vertical structure of existing habitat at La Selva and/or a combination of horizontal and vertical (i.e. multi-dimensional) changes. By using lidar metrics to quantify and map multi-dimensional forest structure, specifically including understory structure, across La Selva and relating those metrics to presence data for understory

insectivores, we may be able to better understand the relationship between multi-dimensional forest structure and habitat suitability for this group.

2.1 Goal and Objectives

The goal of this research is to investigate the relationships between understory bird presence and diversity and multi-dimensional forest structure variables, and to test the ability of lidar to derive forest structure variables in a moist tropical forest. The approach involved developing a number of metrics from primarily lidar data supplemented by selected ancillary spatial data, and the development and testing of bird habitat models and lidar models. This effort was carried out within the following four objectives: 1) acquire bird presence data based on existing long-term records and identify a set of UI bird species of interest associated with La Selva Biological Station, Costa Rica; 2) develop a combination of forest field data and lidar data, and evaluate the correlation between field measurements of aspects of understory structure which UI species are likely to respond to and estimates of understory density and multi-dimensional forest structure derived from airborne lidar data; 3) predict and interpret the distributions of selected understory bird species across the protected area using lidar-derived multi-dimensional forest structure metrics (including metrics related to understory) and other environmental predictors derived from remote sensors, and 4) develop and parameterize a physical lidar model which can be used to test the sensitivity of airborne lidar to understory structure in a dense, closed-canopy tropical forest.

3 STUDY SITE

La Selva Biological Station is a 1536 ha preserve in the Caribbean lowlands of northeastern Costa Rica (10° 26' N, 83° 59' W). Its landscape is comprised of a mixture of primary and secondary tropical moist forest, in addition to agroforestry plots and abandoned pasture. Over the last several decades, the area surrounding La Selva has transitioned from nearly unbroken forest to a matrix of pasture and cultivated land (Figure 1). Apart from the forested southern boundary La Selva shares with Braulio Carrillo National Park, the site has become isolated from other forest fragments by agricultural lands. Braulio Carrillo National Park protects more than 47,000 additional hectares, of which over 90 percent is primary tropical forest. Together, La Selva and Braulio Carrillo form an elevational transect ranging from 26 meters to 2900 meters above sea level in just 20 km. The combined reserve is home to over 500 bird species and more than 5,000 species of vascular plants, of which more than 700 species are trees (McDade 1994). The area of interest (AOI) for this study includes parts of both La Selva and Braulio Carrillo (Figure 1), including both primary and secondary forest. The AOI encompasses all of the vegetation plots and avian point count locations used in the study.

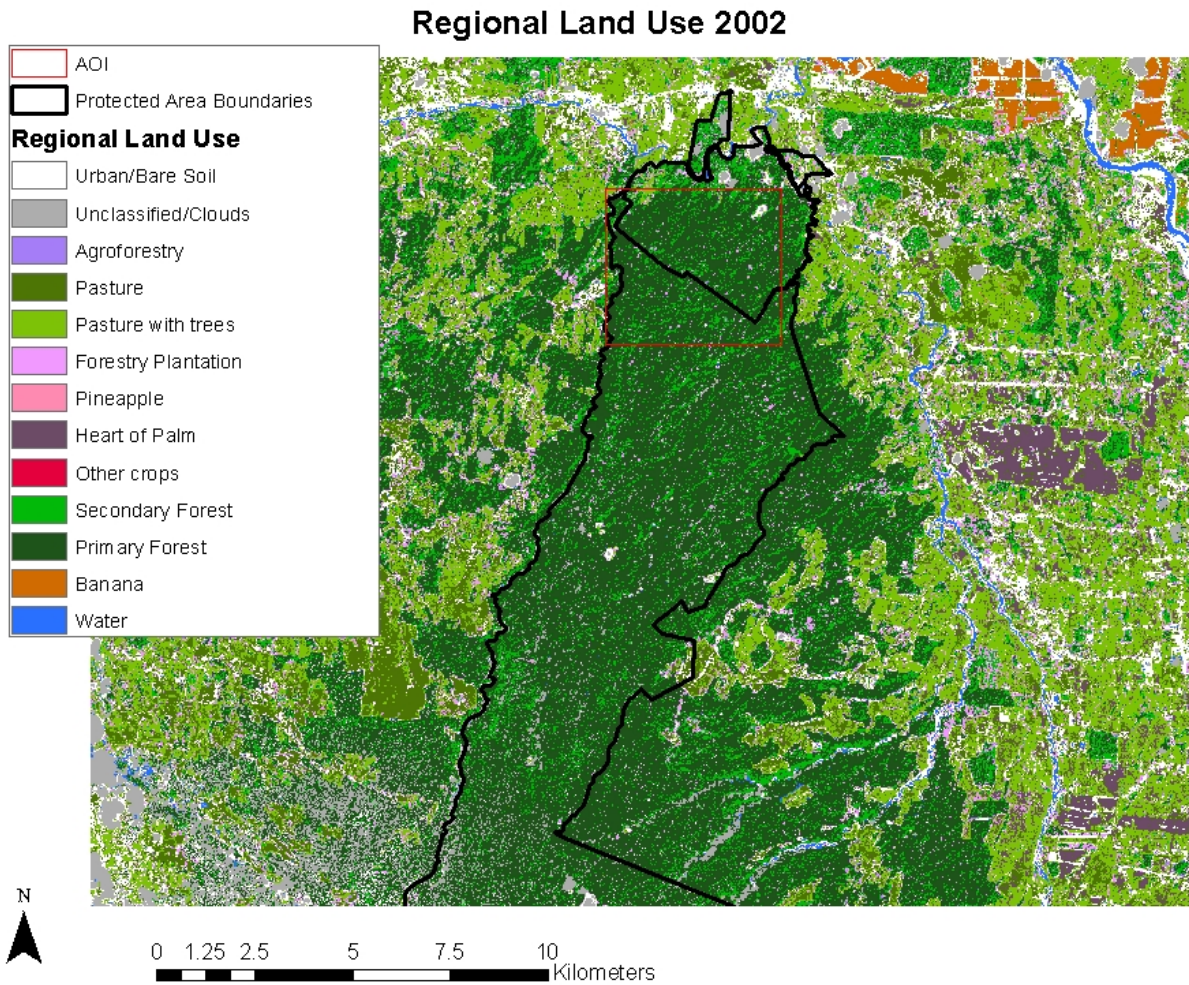


Figure 1. Regional land use for the La Selva area and boundaries of the La Selva / Braulio Carrillo protected area and the study area of interest (AOI).

The La Selva forests feature clumped vegetation strata, with dense tangles canopy material and lianas, compact stands of understory palms and bamboo, and scattered treefall gaps. The degree of canopy closure near ground level is among the highest measured for tropical forests at an average of 98-99% (Fetcher 1994, Nicotra et al. 1999).

4 DATA AND METHODS

The steps involved in data and methodology for this study can be summarized as 1) acquisition of bird and forest field data and creation of variables derived from that data; 2) acquisition of lidar data and creation of variables derived from that data; 3) analysis of the relationship between field and lidar data; 4) development and testing of UI bird habitat models; and 5) parameterization of fractal tree models.

4.1 Field Data

4.1.1 Forest Field Data

Field data on La Selva forest vegetation were needed both as ground truth for comparing with lidar waveforms and for parameterization of a physical lidar model. We utilized forest inventory plots that had been acquired in the course of previous efforts to characterize various aspects of forest structure at the site as well as additional data collected in the field to meet the needs of this study.

This study drew on two existing sources of stem-mapped forest plots (Figure 2). Data used were collected as part of the Tropical Ecology Assessment and Monitoring Network (TEAM)'s Volcán Barva study (Clark 2010) and for the Bosques Project (Redondo-Brenes 2001). TEAM vegetation data included tree or palm species, DBH (diameter at breast height), position within the plot, and condition for each stem ≥ 10 cm and 1.3 m high. Bosques data included species, location, and DBH information for all stems ≥ 5 cm. Both datasets span several years. The year of available field data closest in time to the 2005 collection of lidar data was used for each dataset (2005 for TEAM and 2004 for Bosques data). The TEAM plots were located in primary forest, one at the center of each 1 ha block used for avian point counts, while Bosques plots were located in secondary forest. All stem diameters were measured either at breast height (1.37 m) or, when necessary, above buttressing. We estimated tree heights based on DBH plus maps of forest type and soil type provided by the La Selva GIS Lab (Drake et al. 2002b).

Field understory density estimates were collected specifically for this project in December and January of 2010-11 using a foliage density pole. Estimates were made at a subset of the bird point count locations, across a regular grid within the TEAM forest inventory plots, and at a number of locations between the two TEAM plots. A two meter high, self-supporting PVC pole was marked in alternating 0.1m black and white sections (Toledo et al. 2008). This pole was erected 10 meters from the center of the sample location in each of the cardinal directions and examined by an observer with binoculars standing at plot center (Barlow and Peres 2004). Readings were taken according to the number of pole sections which were clearly visible. The mean of the estimates taken in the four cardinal directions was used as a measure of understory openness.

La Selva Field Vegetation Plots

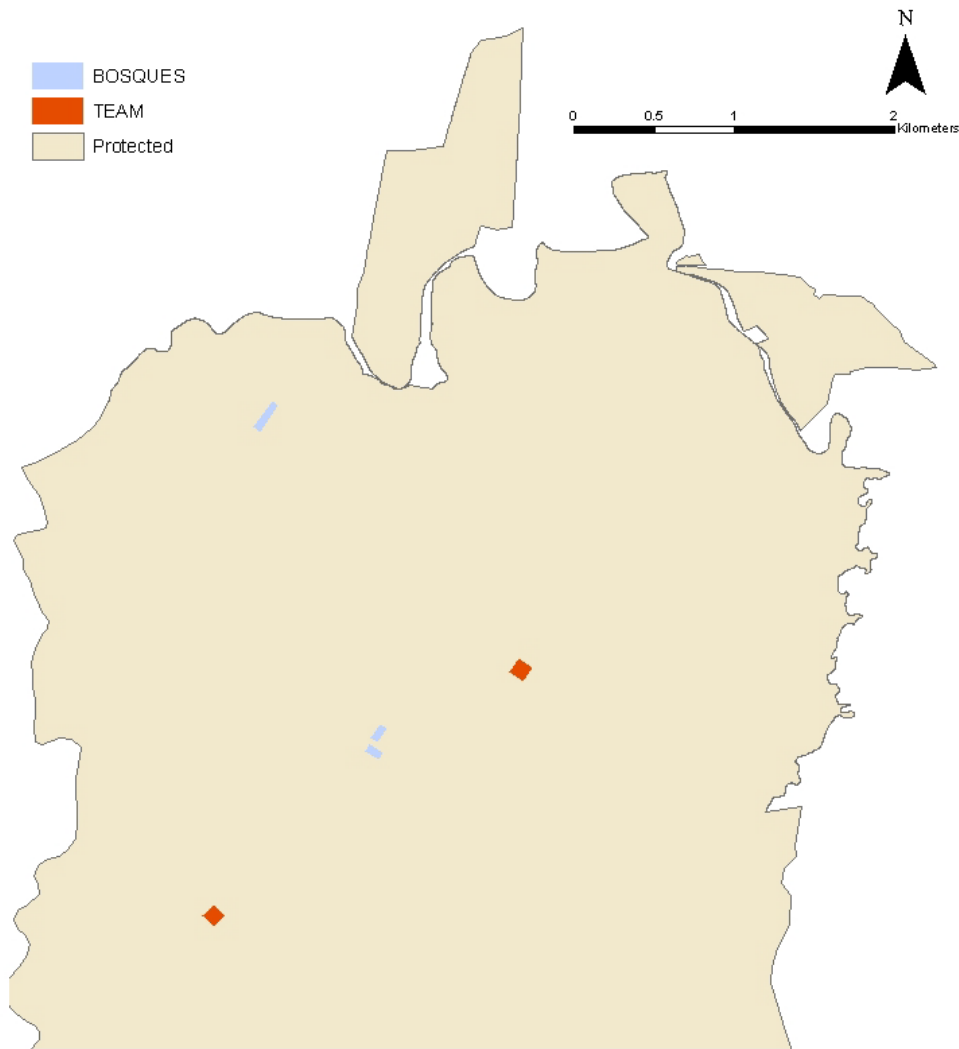


Figure 2. Locations of forest inventory plots within the protected area.

4.1.2 Bird Data

All bird observations were acquired by the Tropical Ecology Assessment & Monitoring (TEAM) Network (Aparicio 2009). TEAM monitoring took place within two separate 1 km² blocks, one within La Selva and one within Braulio Carrillo. Each block consists of six 1 km long transects, located 200 m apart. Each of these transects has six locations for conducting point counts, also set at 200 m intervals, for a total of 36 points per block. Quarterly monitoring data for both blocks was available for fall 2004 – summer 2009. During this date range, monitoring was conducted four times per year. Point counts were recorded for 10 minutes using a combination of audio and visual observations. Counts were completed between sunrise and 9:30 a.m. Observations were tagged with distance classes: less than 10 m, 10-25 m 25-50 m, >50 m or

flyover. Flyover and >50 m observations were not used for modeling in this study. We separated species similarly to Sigel et al., classifying them into 5 habitat guilds (open, forest generalist, understory generalist, understory specialist, canopy/edge specialist) and 5 feeding categories (vegetarian, arthropods/other, insectivorous, carnivorous, omnivorous) (Sigel et al. 2006).

We calculated species diversity for insectivorous understory birds for each TEAM point count location. Habitat quality was also assessed for selected individual UI species of interest. Selected UI species of interest were chosen for inclusion in our study based on a decline in abundance, specifically a change from abundant or common in 1960 to uncommon in 1999 (Sigel et al. 2010), as well as the availability of enough field observations to adequately model the species. Four species were chosen for modeling: the Streak-crowned Antvireo (*Dysithamnus striaticeps*), Tawny-faced Gnatwren (*Microbates cinereiventris*), Plain-brown Woodcreeper (*Dendrocincla fuliginosa*), and Spotted Antbird (*Hylophylax naevioides*).

4.2 Lidar and Other Spatial Data

4.2.1 LVIS Data and Creation of Lidar Metrics

Lidar data was collected in 2005 over La Selva and Braulio Carrillo by the Laser Vegetation Imaging Sensor (LVIS), an airborne large footprint, full-waveform sensor (Blair 1999). Full-waveform sensors hold several advantages over the discrete return lidar sensors which have been used for much of the previous work on lidar sensing of forest structure. Full-waveform lidar sensors digitize the entire return signal from each laser pulse, in contrast to discrete return sensors, which record only one or a few returns for each pulse (Dubayah 2000). As a result, small changes in the volume of vegetation can influence the shape of the return waveform in a full-waveform sensor, whereas with discrete return systems, just one or a few of the strongest return pulses are recorded (Lim et al. 2003). Discrete return sensors also generally have a much smaller footprint on the ground for each pulse (typically under a meter), while typical full waveform footprints are on the order of several to tens of meters.

LVIS data for the La Selva area was collected at an altitude of 10 km and is available through the Goddard Space Flight Center (GSFC). Nominal footprint diameters were 25 m, with overlapping of flight paths resulting in an average spacing of approximately 15 m between footprint centers. The return signal is digitized so that each bin of the waveform represents a vertical stratum of 30 cm. Waveforms were generally geolocated to within 2m or better (Blair and Hofton 1999). In addition to the raw waveform data, GSFC provided several metrics calculated for each laser shot, including the elevation of the lowest mode within the waveform (assumed to be the ground), and rh25, rh50, rh75, and rh100, representing the heights relative to the ground at which each quartile of the waveform energy occurs. An estimate of the signal mean noise level for each waveform was also provided with the data (Blair 2006).

In order to develop additional metrics from the LVIS data, we first subtracted the signal mean noise level from each raw waveform. We created additional rh metrics beyond rh25, 50, 75, and 100 in order to identify the most useful rh values for model predictions. To create additional rh metrics, the waveform was converted to an upward-directed cumulative distribution. To identify rh(i), the waveform bin at which the cumulative percentage of the total waveform reached i was then referenced to zg, the identified ground return. For low values of i, such as rh30, the proportion of the waveform below zg was often greater than i, resulting in a negative value for rh(i).

Canopy height profiles were also developed from the raw waveforms following Harding et al. 2001. Using the ground returns identified as zg in GSFC data, the end of the ground return pulse was defined as the last signal above the mean noise level. The beginning of the ground return was identified using the ratio between signal end-to-peak and peak-to-start derived from an impulse response for LVIS estimated using returns from known flat surfaces. The ground portion of the waveform was then increased by a factor of 2 to account for the difference in near-infrared (NIR) reflectance between canopy and ground. A cumulative height distribution of the vegetation portion of the return was then normalized by the adjusted total return (vegetation + ground*2). Occlusion of the laser beam by higher canopy layers was corrected for by weighting the distribution by $[-\ln(1-\text{closure})]$, which is the MacArthur-Horn transformation (MacArthur and Horn 1969). Finally, the distribution was normalized and converted to an incremental height distribution, resulting in a canopy height profile (CHP) representing fraction of total plant area per waveform bin. Drake et al. (2002) found good agreement between CHPs developed with this method and vertical canopy profiles derived from modeled field data (Drake et al. 2002b). Relative height metrics were then calculated using the transformed canopy height profile (chprh in Table 1) in the same way that rh metrics were calculated from the raw waveform.

Three higher-level lidar metrics developed by previous studies were calculated from the LVIS data in addition to rh and chprh values. Canopy cover was estimated as the proportion of the adjusted total return represented by vegetation, or $[\text{vegetation} / (\text{vegetation} + \text{ground} * 2)]$ (Means et al. 1999). We also calculated a vertical distribution ratio (VDR; Goetz et al. 2007) defined as $[(\text{rh}100 - \text{rh}50) / \text{rh}100]$. Finally, a lidar-based version of foliage height diversity (FHD) was calculated to represent the evenness of vertical foliage distribution (MacArthur and MacArthur 1961). A lidar-derived FHD uses the same Shannon-Weiner index (H') to account for both total foliage density and its distribution, where $FHD = -\sum f_i \log f_i$; where $f_i = d_i / D$; where d_i = the density of foliage in layer I; and where D = the total density of foliage over all layers in the vertical profile. However, rather than arbitrarily defined layers measured in the field, a lidar-derived FHD measures distribution across the i waveform bins represented in the CHP.

Once created, lidar metrics were transformed from dense footprints into continuous raster surfaces for use in modeling. Lidar footprint locations were imported into ArcGIS and attributed with the calculated lidar metrics. Footprint data was then converted from shapefiles to terrain

datasets. A terrain dataset is a set of vector-based measurements and rules that allow the generation of surface models. A series of data points stored as X, Y, and Z values is used to partition a geographic area into continuous, non-overlapping triangles, a surface generally known as a triangulated irregular network (TIN) (Childs 2004, Kearns 2005). The continuous surfaces of the terrain datasets were then interpolated to rasters. Raster cell size was chosen based on average spacing between lidar footprints. Conversion to a terrain first, and then to a raster helps to compensate for the irregular distribution of lidar footprints by allowing a more accurate interpolation compared to block models (Shorter 2005).

4.2.2 Ancillary Spatial Data

We used an existing GIS layer containing a set of professionally surveyed elevation points to assess the accuracy of the ground elevations estimated from LVIS data (Figure 3). These 8798 elevation measurements were collected during the survey for the La Selva grid system. Ancillary GIS data created by the La Selva GIS Lab was also used to describe land uses in the region, identify the soil types of forest inventory plots, and determine the locations of primary vs. secondary forest. We used the provided land-use data to map the distance to the nearest abrupt forest edge (e.g., forest-clearcut, forest-field and forest-road edges) across the protected area. Using the ArcGIS Spatial Analyst extension, we created a raster for which each cell contained the Euclidean distance to the nearest edge of the forest patch in which it was located.

Table 1. Multi-dimensional habitat structure variables used in modeling

Variable	Description
zg	Elevation of the lowest detected mode within the waveform
slope	Steepness of the DEM developed from zg
rh(i)	Height relative to zg at which i% of the waveform energy occurs
chprh(i)	Height relative to the start of the ground return at which i% of the total area of the CHP occurs
chp 0-1.5, chp 0-3, chp 0-6	Percentage of the area of the CHP occurring within 1.5, 3, and 6 m of the start of the ground return
cover	Vegetation returns / (Vegetation returns + Ground returns*2)
distance to forest edge	Distance to the nearest boundary of the forest patch
FHD	Foliage height diversity, a measure of canopy layering
VDR	Vertical Distribution Ratio, (rh100-rh50)/rh100

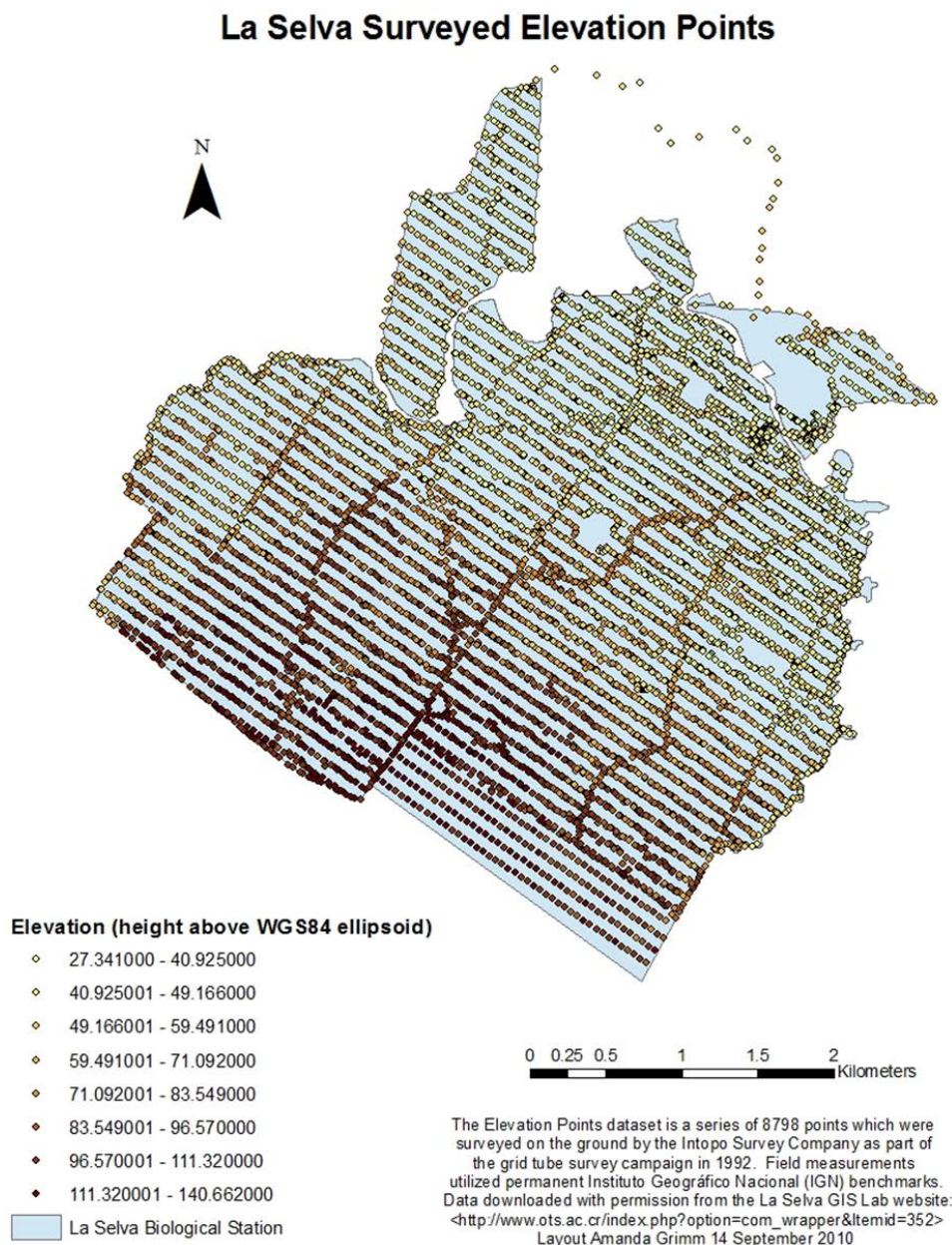


Figure 3: Surveyed elevation points for La Selva.

4.3 Relating Lidar Metrics to Field Data

Field data on understory structure included both the estimates of understory openness collected using a foliage density pole and rough estimates of understory density based on the biomass of trees ≥ 10 cm, estimated based on DBH as described in section 3.1.1. An earlier study at La Selva found that LVIS lidar data could be used to estimate above-ground biomass fairly accurately (Drake et al. 2002a), and understory biomass may be a good indicator of habitat suitability for UI species (Jullien and Thiollay 1998). Field estimates of understory biomass were also utilized to parameterize the physical lidar model. Typically, estimates of above-

ground biomass (AGB) use only stems with a DBH of ~10cm or greater, omitting small-diameter understory stems as their contribution to total biomass is assumed to be negligible (Gerwing et al. 2000). In order to estimate understory biomass, we established proportional relationships between overstory biomass and understory biomass. For the TEAM plots, representing primary tropical forest, understory biomass was estimated as 3.8% of overstory biomass based on an earlier study of primary forest at La Selva where all trees and palms 1 cm or more in diameter within 10x50m transects were measured (DeWalt and Chave 2004). For the Bosques plots, comprised of tropical secondary forest, estimates of the biomass of stems with a DBH of 5-9.9cm measured within the Bosques plots (Chambers et al. 2001) were multiplied by 1.5 to account for stems of DBH 1-4.9 (Nascimento and Laurance 2004), resulting in an average understory biomass of 8% of overstory biomass. This estimate is similar to the Nascimento study, which showed that understory live biomass made up about 9.2% of large tree biomass.

Foliage density pole field measurements and calculated estimates of understory biomass were compared to each other and to five lidar-based metrics with the potential to provide information on understory biomass: rh25, chprh10, chprh20, chp 0-1.5, and chp 0-3 (Table 1). Because the estimates of understory biomass were strongly left-skewed, they were scaled between 0 and 1 and normalized by $\log[X/(1-X)]$ before making comparisons (Rummel 1970). The accuracy of the DEM we constructed from LVIS data was also evaluated in comparison to the field-surveyed grid of elevation points (both measured as height above WGS-84 ellipsoid) in order to gauge the accuracy of the identified LVIS ground returns.

4.4 Bird Distribution Analysis

4.4.1 Modeling Diversity of Understory Insectivores

Statistical summaries were made of the calculated lidar metrics for the footprints falling within 50 m of each point count location, 50 meters being the maximum distance used for recording bird observations when the point counts were performed. Footprints falling partly within the 50 m radius circle were weighted by the percentage overlap. A multiple linear regression (MLR) was then constructed to assess linear trends between the lidar metrics associated with each point count location and the UI diversity observed there. The best MLR model was chosen using Akaike's Information Criteria (AIC) in a stepwise algorithm, using the stepAIC function from the MASS package in R (Team 2008). The model used both forward and backward selection in order to produce the most complex model possible without overfitting. The initial model contained all of the lidar variables; each variable in turn was then removed and potential improvements to the model which could be made by including previously removed variables were assessed. The final model minimized AIC, which compromises between model fit and complexity. Predicted UI diversity could then be mapped across the study area. K-Fold cross-validation was used to evaluate the regression, where the 72 point count locations were divided into six subsets and the regression was recalculated six times. Each time, one of the six subsets

was used as the test set and the other five subsets were put together to form a training set. Then the mean squared error (MSE) for each fold was summed, divided by the number of observations, and the square root was taken to get the cross-validated standard error of the model.

4.4.2 Models of Suitable Habitat

Models of habitat suitability for individual UI species were developed in MaxEnt using the rasters of the lidar variables and of distance to forest edge as the environmental layers (Table 1), and bird point count locations where a particular species had been observed as the sample data. Maximum entropy is a general purpose machine learning method that makes predictions based on incomplete information, harnessed in the MaxEnt program for inductive modeling of wildlife presence data (Phillips 2006). MaxEnt has proven capable of producing useful species distribution models with small sample sizes (Hernandez et al. 2006, Pearson et al. 2007). MaxEnt also does not require absence data, which is optimal for the La Selva avian data because understory insectivores tend to be cryptic, and absence reports for these species based on ten minute point counts may not be completely reliable.

MaxEnt estimates the most uniform (maximum entropy) spatial distribution of a possible across the study area given the constraint that the expected value of each environmental variable under this estimated distribution matches its empirical average. The program starts with a uniform probability distribution and iteratively alters the weight of one variable at a time to maximize the likelihood of the occurrence dataset. The maximum entropy algorithm is guaranteed to converge to the optimum probability distribution, and because it does not use randomness, the outputs are deterministic (Hernandez et al. 2006). We used the cumulative output format for MaxEnt, which represents the prediction for each analysis cell as the sum of the probability value for the current analysis cell and all other cells with equal or lower probability values, scaled from 0 to 100. The cell with a value of 100 is considered the most suitable, while cells close to 0 are the least suitable within the study area (Phillips 2006).

4.4.3 Model Testing

Because the numbers of observation locations available for each species were relatively small, we evaluated model results using the jackknife validation approach developed by Pearson et al. (2007). For a species with n observations, n models were built, removing each observation point once from the set of data and running the algorithm using the remaining $n - 1$ sample points. Evaluating the model then became a matter of how many of the iterated models correctly predicted the excluded locality. The test statistic D was formulated as $D = \sum X_i(1 - P_i)$; where X_i equals 1 if the excluded point is predicted as a presence location and 0 if it is not; and P_i = the proportion of the study area predicted to be habitat having excluded the test point. The software program developed by Pearson et al. (2007) was used to calculate the P value representing the probability that model success was not better than a random assignment of 0 or 1 to X_i . This

method assigns a greater weight to successful predictions of excluded points when the proportion of the study area predicted to be habitat is lower.

Because MaxEnt predictions of habitat suitability level are continuous, it is up to the user to define a ‘decision threshold’ above which the model output is assumed to represent species presence and below which represents unsuitable habitat. For each species model, we overlaid the observation locations onto the prediction map created by MaxEnt to find the map pixel with the lowest prediction value actually containing an observation; i.e., the lowest habitat suitability level MaxEnt assigned to a true observation from the training set. This lowest prediction value was then defined as the decision threshold for that species. This choice of decision threshold is referred to elsewhere as the ‘lowest presence threshold’, or LPT (Pearson et al. 2007). This method of setting the threshold is both conservative, as the only raster cells predicted as suitable habitat are those at least as suitable as one of the recorded observations, and ecologically intuitive.

4.5 Fractal Tree Models

Over the past years we have developed several forward models for remote sensing applications (Yi-Cheng and Sarabandi 1999, Sarabandi and Lin 2000). Recently, we have focused on enhancing our capabilities for better understanding lidar (and radar) backscatter on forested landscapes through development of our fractal tree model software. We parameterized fractal models which can represent the structure and dimensions of specific tropical tree species, both for visualization purposes and for eventual incorporation into a physical-based forward model currently in development. The forest stands created by the fractal tree software include a simulation of every branch, needle, and leaf, its position, orientation, length, diameter, thickness, moisture, and bulk density. These types of models can be used to explore: 1) how well one might expect the LVIS lidar data to represent the actual understory and 2) what level of understory biomass is needed for the understory signal to be reliably captured by LVIS or similar lidars.

Fractal tree models were parameterized for all tree species identified within TEAM and Bosques plots at La Selva using fractal-based L-systems. These inputs were generated via a fractal tree model software program developed for other forest modeling efforts (Yi-Cheng and Sarabandi 1999). The La Selva fractal models were parameterized based on information found in the literature on growth form (e.g. treelet, midstory tree, tall tree, or palm) and maximum heights for each species (Appendix 1). Photos of each species were utilized to better model the fractal representations.

The fractal tree model works by recursively growing and splitting the branches of a model tree n times. The user specifies n for a specific species based on the complexity of the particular tree’s structure. The trunk and branches of the tree are modeled by stratified dielectric cylinders, and leaves are modeled by dielectric disks above an arbitrary tilted plane (the ground). The cross

section and the length of younger branches decrease as the branching process progresses. The parameters we defined for each fractal model include trunk tilt angle, leaf density, leaf radius, branching and growth pattern, both a tilt angle and a rotation angle to define the relationship between a new branch and its parent, degree of randomness, and number of iterations of the fractal branching/growth pattern (Yi-Cheng and Sarabandi 1999).

Tropical forests contain specific types of vegetation not found in temperate systems, which our existing fractal tree model cannot yet fully account for. Features such as woody lianas and specialized buttressed or stilt roots were not represented in our fractal simulations.

5 RESULTS

5.1 Lidar Metrics of Forest Structure

The field estimates of understory density obtained using a foliage density pole were compared to several lidar metrics (chp 0-1.5, chp 0-3, chprh10, chprh20, and rh25). The only significant correlation was between the density measurements and rh25 ($p = 0.010$), but even that relationship was weak (Figure 4). Estimated understory biomass was compared to the same lidar metrics with no significant correlations. When the relationship between foliage density and understory biomass was examined, a small but significant correlation was found (Pearson correlation coefficient of -0.224 , $p=0.018$). All correlation coefficients are listed in Table 2.

When lidar estimates of elevation are compared to the 5039 independent measurements from ground-based surveying which fell within the area of interest, the mean elevation difference is less than a meter (0.73 m), with a standard deviation of 3.69 m.

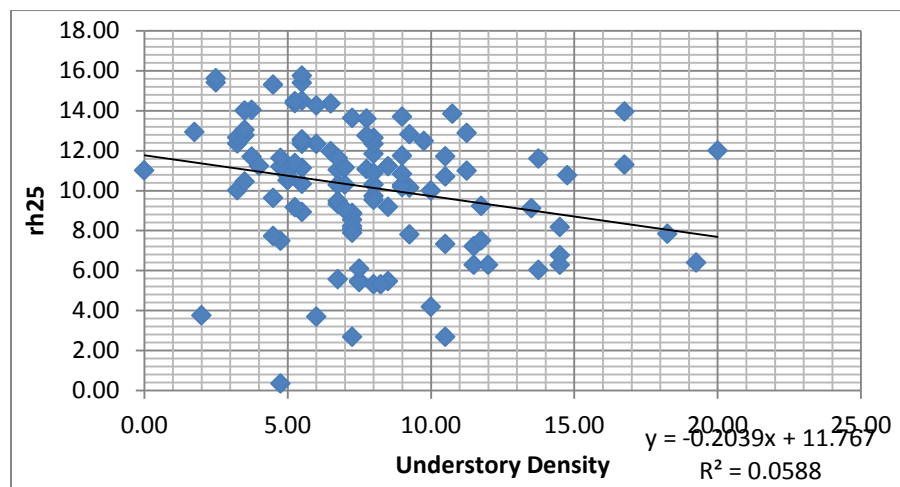


Figure 4. Field estimate of understory density vs. rh25.

Table 2. Correlations between field and lidar-based estimates of understory structure.

	Density	Biomass
rh25	-0.243 (0.01)	-0.035 (0.80)
chprh10	0.022 (0.82)	-0.057 (0.68)
chprh20	-0.121 (0.20)	-0.114 (0.40)
chp 0-1.5	0.050 (0.60)	0.187 (0.17)
chp 0-3	0.010 (0.92)	0.230 (0.09)
Density	--	-0.224 (0.02)
Biomass	-0.224 (0.02)	--

5.2 Bird Distribution Models

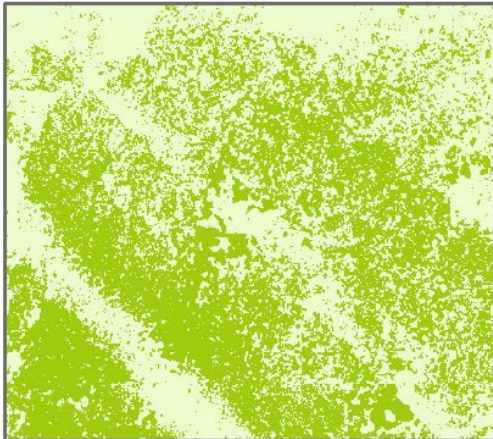
MaxEnt models were developed for four species of understory insectivore. Projected potential distributions using the lowest presence threshold (LPT) are presented in Figure 5. In each case, the model was trained using all observation locations. High success rates (i.e. low rates of omission for excluded variables) were obtained for all species, and statistical significance was obtained during testing for all species except the Streak-crowned Antvireo (Table 3).

Environmental variables which contributed at least 5% of the gain in the model were considered significant predictors, while those which contributed at least 10% were considered very significant. Of the 31 environmental variables used for model development (Table 1), only 11 were significant contributors to any of the four models. Each species model had between 4 and 8 significant contributors, and between 2 and 5 very significant contributors (Table 4). The only variable to emerge as very significant for all species was percent canopy cover. Distance to forest edge was significant in all models and very significant in 3 out of 4.

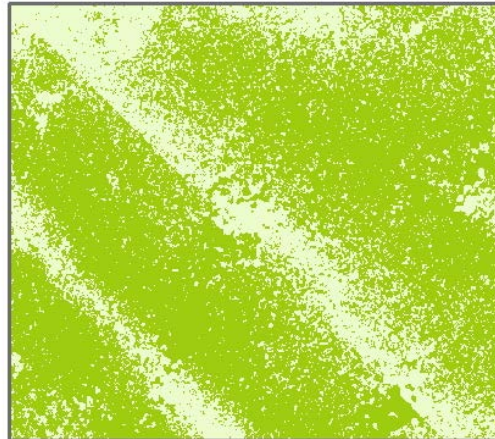
Table 3. Results of jackknife validations of MaxEnt models.

Species	Observations	Success rate	p-value
Plain-brown Woodcreeper	26	0.846	0.000
Streak-crowned Antvireo	31	0.742	0.230
Spotted Antbird	19	0.778	0.003
Tawny-faced Gnatwren	14	0.857	0.000

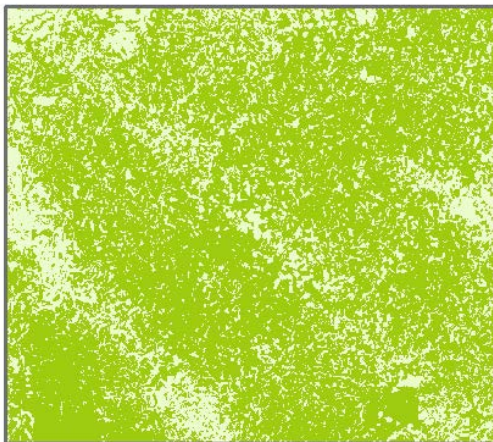
Plain-brown Woodcreeper



Streak-crowned Antwreio



Spotted Antbird



Tawny-faced Gnatwren

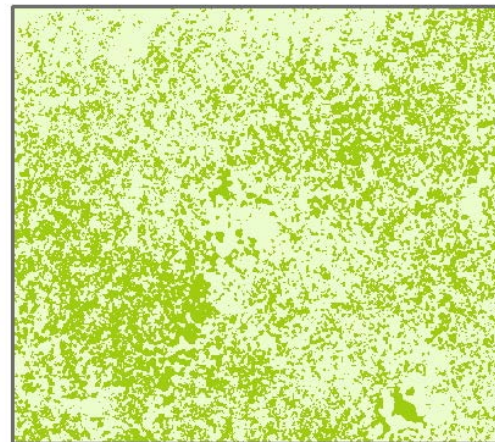


Figure 5. MaxEnt projections of distribution of potential habitat for four bird species of interest across the study area

Table 4. Environmental variables which contributed significantly to each species model. DENFUL = Plain-brown Woodcreeper; DYSSTR = Streak-crowned Antwreio; HYLNAE = Spotted Antbird; MICCIN = Tawny-faced Gnatwren.

	DENFUL	DYSSTR	HYLNAE	MICCIN
Very Significant	cover	cover	cover	cover
	distedge	distedge	distedge	fhd
	rh100		zg	chp_0_15
	zg		slope	
	chprh10			
Significant	fhd	fhd	rh100	distedge
	chprh90	chprh90		
	rh40	rh40		
		chprh50		
		chp_0_15		
		rh100		

5.3 Fractal Tree Models

A fractal model was created for each of the 194 tree species found in the TEAM and/or Bosques vegetation plots. The same model was sometimes used for similar species in the same genus. The fractal models can be used in combination with the specific information on tree locations and sizes from the stem-mapped vegetation plots to simulate actual forest plots (Figure 6). Because the TEAM and Bosques datasets only contain information on stems above a minimum DBH (10 cm for TEAM and 5 cm for Bosques data), the simulated forest plots are lacking the small stems that make up much of the live biomass of the understory strata.

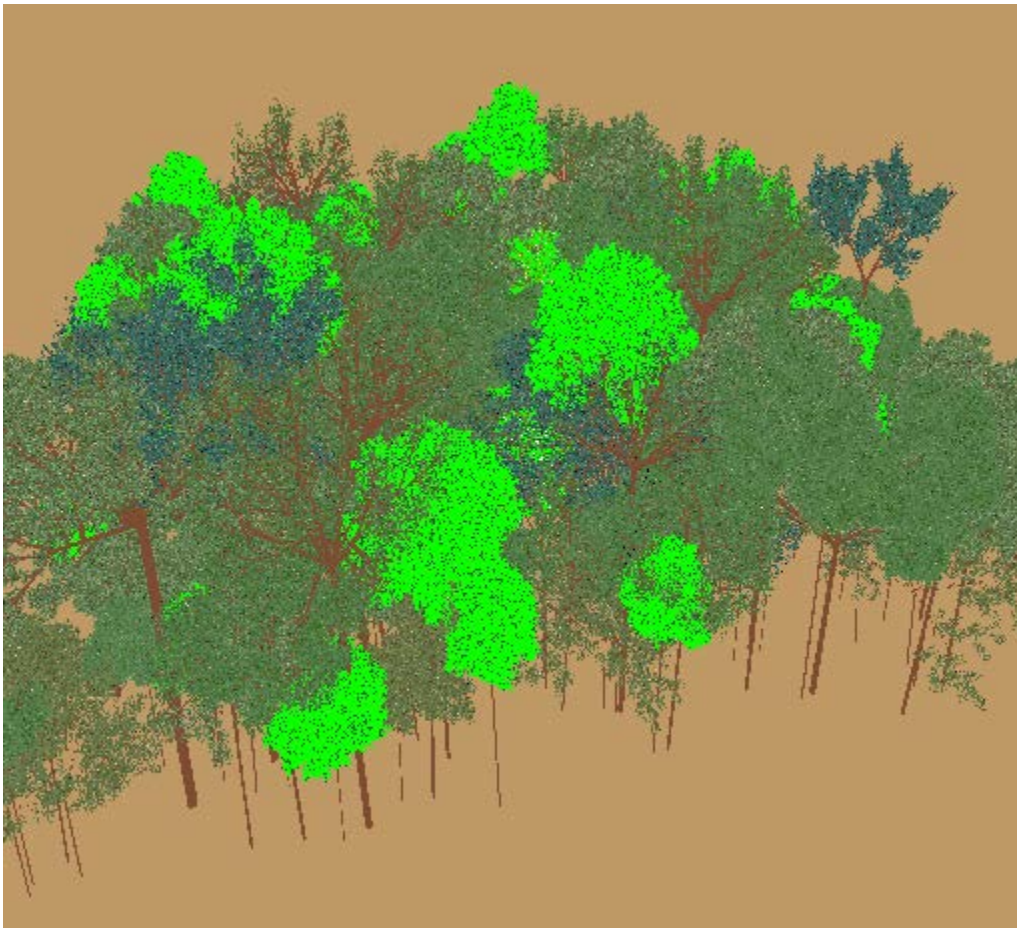


Figure 6: Fractal model of TEAM vegetation plot 1.

6 DISCUSSION

6.1 Lidar vs. Field Metrics

Field estimates of understory density and understory biomass were weakly correlated, but each correlated most strongly to different lidar metrics. The relationship between understory density and rh25 was intuitive, in that a denser understory resulted in a lower value for rh25. A lower

rh25 relative to rh100 generally indicates that a greater proportion of the biomass in the vertical profile is concentrated closer to the ground. Estimated understory biomass was moderately and near-significantly ($p=0.09$) correlated with the proportion of the canopy height profile occurring between 0 and 1.5 meters above the ground (chp0-1.5). Multiple earlier studies found good general agreement but significant statistical differences between field- and lidar-derived canopy height profiles, which may weaken relationships between CHP metrics and field data (Harding et al. 2001, Drake et al. 2002b). Still, given the extremely high degree of canopy closure near the ground observed for this site in this and earlier studies (Fetcher 1994), the ability of a lidar metric to even weakly predict biomass in the understory strata is noteworthy.

Our lidar-based estimates of ground elevation were more accurate than those developed by an earlier study ($0.73 \text{ m} \pm 3.69$ vs. $2.54 \text{ m} \pm 5.03$), which may be related to only using the subset of field elevation measurements which fell within the study area or to our method of interpolating the waveform data to a DEM (Hofton et al. 2002).

6.2 Maxent Models

In (Drake et al. 2002b), untransformed metrics were equivalent to CHP metrics in ability to predict estimated above-ground biomass (EAGB) via stepwise multiple regression. Our results showed a similar equivalency between the two in predicting understory density and biomass, but metrics derived from canopy height profiles were selected for inclusion in MaxEnt models at a higher frequency than metrics from the untransformed waveforms, and made more significant contributions to model performance. This suggests that transformed canopy height profiles may be better at capturing information on aspects of the 3D distribution of vegetation to which understory birds respond.

Insectivorous understory birds are known to be highly specialized with regards to diet and foraging behavior (Şekercioğlu et al. 2002, Sodhi et al. 2004, Lindell et al. 2007). The four species modeled here alone display a diversity of preferences for foraging microhabitat and food capture techniques; the Streak-crowned Antwren sallies from its perch to glean prey from vegetation, while the Plain-brown Woodcreeper follows army ants, picking off the arthropods flushed by the swarm (Willis 1972a, Schulenberg 1983). The Spotted Antbird prefers a fairly open understory where it can locate prey on the ground, rarely foraging more than 2 m above the ground, while the Tawny-faced Gnatwren is drawn to treefalls, and is most often observed foraging in vine tangles along the edges of interior forest gaps (Willis 1972b, Schemske and Brokaw 1981). Any change in land use or management which alters the structure of the understory strata at which these birds forage, nest and roost could impact the area's suitability as habitat.

The MaxEnt models for these species were limited by the nature of the bird observation data available for the site (quarterly observations at predefined locations), but still revealed some similarities and differences between species in terms of which lidar metrics were most useful for

predictive modeling. Percent canopy cover and distance to forest edge stood out as important characteristics across all species. Interestingly, increasing canopy cover correlated positively with increased habitat suitability for three of the species but negatively with suitability for the Tawny-Faced Gnatwren, the gap-foraging specialist. Suitability for two other species had a generally positive correlation with cover which dropped off again at very high cover values (Figure 7).

All species responded favorably to increasing distance to the forest edge, which aligns with the existing view that this guild avoids manmade forest edges (Laurance 2004). Within this study, only abrupt edges were considered, such as the boundaries between forested areas and fields, plantations, roads, etc. UI response to this type of edge is better documented than response to interior edges or gradual edges, such as where a forest transitions into shrubland (Lindell 2007), and the location of an abrupt edge is more clearly defined. While UI bird species did exhibit a response to abrupt edge, future studies could look more closely at the effect of transitional zones and gap-related forest patchiness on presence of individual species.

Apart from those commonalities, some species but not others responded to elevation, slope, canopy height, foliage height diversity, a few different CHP metrics describing the density of the understory, and rh40. A metric selected as very important for one species was often not utilized to any significant degree in the model for another. A model of habitat suitability for the understory insectivore guild as a whole might perform reasonably well using only canopy cover, distance to forest edge, and FHD, but would ignore major differences in habitat selection criteria between species.

Habitat suitability maps for all four species of interest portrayed most of the forested habitat as suitable, but with two distinct bands of lower suitability running from the northwest to the southeast of the plot (Figure 5). For the Plain-brown Woodcreeper and Streak-crowned Antwren in particular, these bands were rated as poorly as non-forest in terms of habitat suitability. Looking at the input environmental layers, forest in these bands tends to have more gaps, lower canopy height, and lower values for many derived lidar metrics, but the final models show more distinct bands than any one of the input maps. The primary band of lower suitability runs along the border between La Selva and Braulio Carrillo, which happens to be a band of secondary forest between two areas of primary forest. Cleared forest between Braulio Carrillo and La Selva was purchased in the 1980s and has been allowed to regrow to increase the connectivity between the properties (McDade 2004).

While canopy cover and distance to forest edge have not changed over the time span in which understory insectivores have declined at La Selva, it is possible that foliage height diversity has. Bird populations could negatively respond to such changes in multi-dimensional forest structure based on their sensitivity to physiological constraints, reduction in prey availability, increased exposure to predators, an understory which is too dense or open for their specific foraging

technique, and/or avoidance of gaps. (Thiollay 1997) Changes in the height distribution of foliage could potentially be occurring due to changes in microclimate due to the logging of surrounding forests, or due to the explosion of the collared peccary (*Tayassu tajacu*) population observed at the site. The peccaries are unusually dense at La Selva, likely due to the loss of large predators and restrictions on hunting. Collared peccaries were rarely observed at La Selva in the 1970's, but their abundance had risen to an estimated 14/km² by 1993, and is likely to be higher than that today (Torrealba-Suárez 1994). The 1993 estimate is substantially higher than any reported from other tropical and temperate environments (Terborgh et al. 1986, Glanz 1982, Aquino et al. 2007, Schweinsburg 1969).

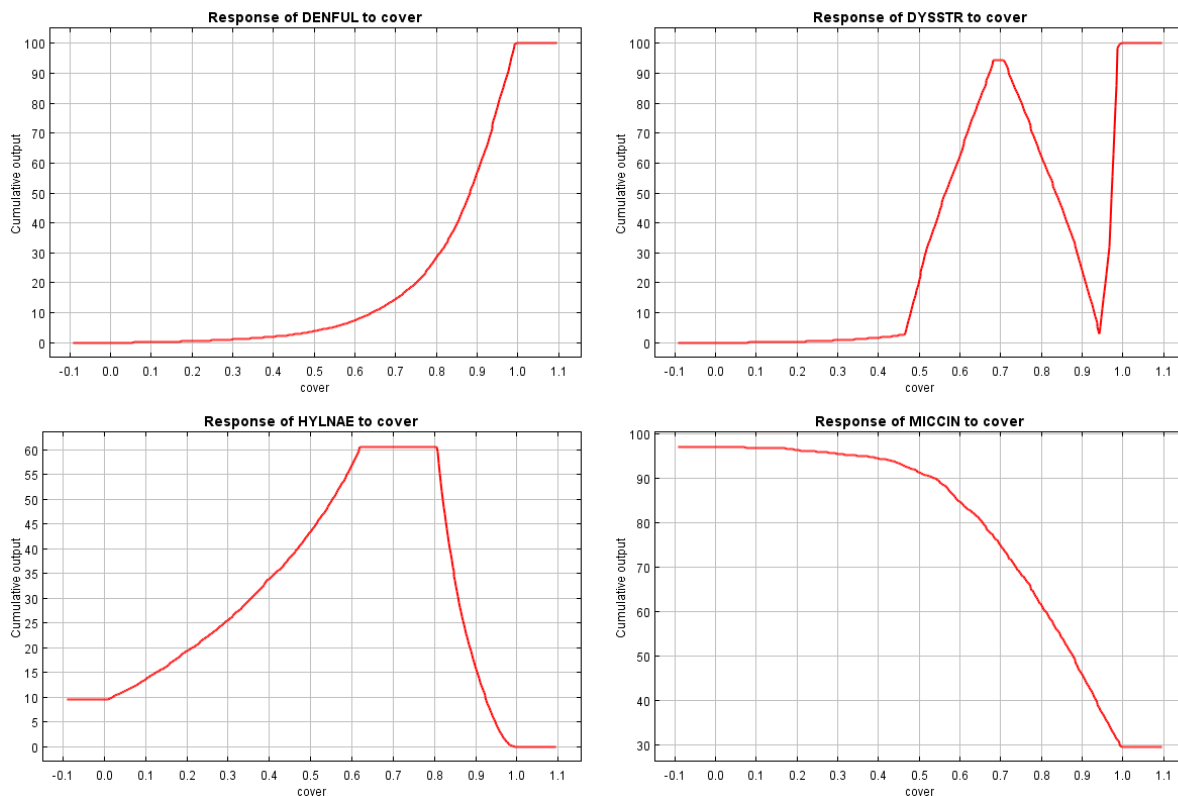


Figure 7. Response of bird species to canopy cover. DENFUL = Plain-brown Woodcreeper; DYSSTR = Streak-crowned Antvireo; HYLNAE = Spotted Antbird; MICCIN = Tawny-faced Gnatwren.

6.3 Ability of lidar to measure forest understory

Previous assessments of understory vegetation with LIDAR have typically been less accurate under dense tree canopies as compared to more open canopies (Maltamo et al. 2005, Goodwin et al. 2006, Skowronski et al. 2007, Su and Bork 2007), due in part to the decrease in the proportion of laser pulses reaching the lower forest strata. In practice, maps or models of multi-dimensional forest structure need to be reliable under different forest density conditions so that spatially consistent ecological inferences can be made.

One major break between this study and earlier work is that much of the previous work on multi-dimensional forest structure involving understory has utilized small footprint discrete-return lidar. While a discrete-return instrument is adept at characterizing the surface of the canopy, it is limited to recording one or a few of the strongest backscatter pulses. In a closed-canopy forest, discrete-return lidar is often unable to detect sub-canopy vegetation except where it can penetrate canopy gaps (Clawges et al. 2008). A full-waveform sensor is more adept at collecting sub-canopy returns. This is because of 1) its larger footprint, which can take better advantage of small breaks in the canopy, and 2) the continuous recording of lidar backscatter at a very high vertical resolution (Weishampel 1996, Lefsky et al. 2002). Overall, the ability of full-waveform sensors to detect smaller amounts of vegetation density within a canopy has the potential to make it more suited to the accurate characterization of multi-dimensional structure in dense forests.

Additionally, here we used the MacArthur-Horn transformation to attempt to account for the occlusion of the lidar beam by upper layers of vegetation. Earlier work on development of canopy height profiles at La Selva using the MacArthur-Horn transformation found that qualitative agreement between field and lidar-derived CHPs was fairly good, and that correlations between the two were high, although significant differences did exist between the two (Harding et al. 2001, Drake et al. 2002b). In that study, transformed CHPs were more similar to field-derived profiles than untransformed waveforms in primary forest, but performed less well than the raw waveforms for secondary forest plots (Drake et al. 2002b). While the transformation to CHPs is a logical way to deal with the problem of occlusion, the MacArthur-Horn transformation assumes homogeneity of horizontal layers, which may create other biases when applied to the relatively clumped strata of our site (Harding et al. 2001).

6.4 Implications for conservation of understory insectivores

After studying bird census data dating back to 1960, Sigel et al. found that insectivores represent at least half of the bird species declining at La Selva, and concluded that La Selva appears to be too small to maintain the understory insectivore guild (2006). Based on the guild's avoidance of forest edges and general need for large home ranges, others have also suggested that protected areas of tropical forest will slowly lose their understory insectivore populations unless the protected area is a large and contiguous forest. The importance of distance to forest edge in our models supports the idea that minimum patch size may be important for maintaining understory insectivore populations, but the significance of structural variables such as FHD, CHPRH10, and CHP 0-1.5 suggests that the multi-dimensional forest structure and, specifically, the condition of a forest's understory may be as important in terms of habitat suitability as the forest's size.

Effective management of forests for protection of diversity requires either information about the presence and abundance of organisms – which is not available or easily obtained for many species – or the development of indicators of habitat quality that correlate with species distributions. At the landscape scale, the multi-dimensional structure of forests can be quantified via lidar and used to significantly improve predictions of the occurrence of some species.

6.5 Ongoing and future work

Further studies are needed to explore the relationship between lidar metrics and understory biomass more explicitly, and to develop a more nuanced approach to transforming lidar waveforms which can account for the clumping of canopy layers. While outside the scope of this study, a better understanding of the life history of understory insectivores would enable us to create models based on known key habitat needs of individual species rather than the inductive method used here.

One substantive way to advance this type of study would be to develop an independent method for quantifying the uncertainty in lidar metrics. We are currently involved in building a physical lidar model with which to simulate lidar returns from field sites and better understand patterns of lidar backscatter. The fractal tree models created from the data used in the work presented here can be used to test lidar models, leading to their refinement and utility for lidar measurement of tropical understory.

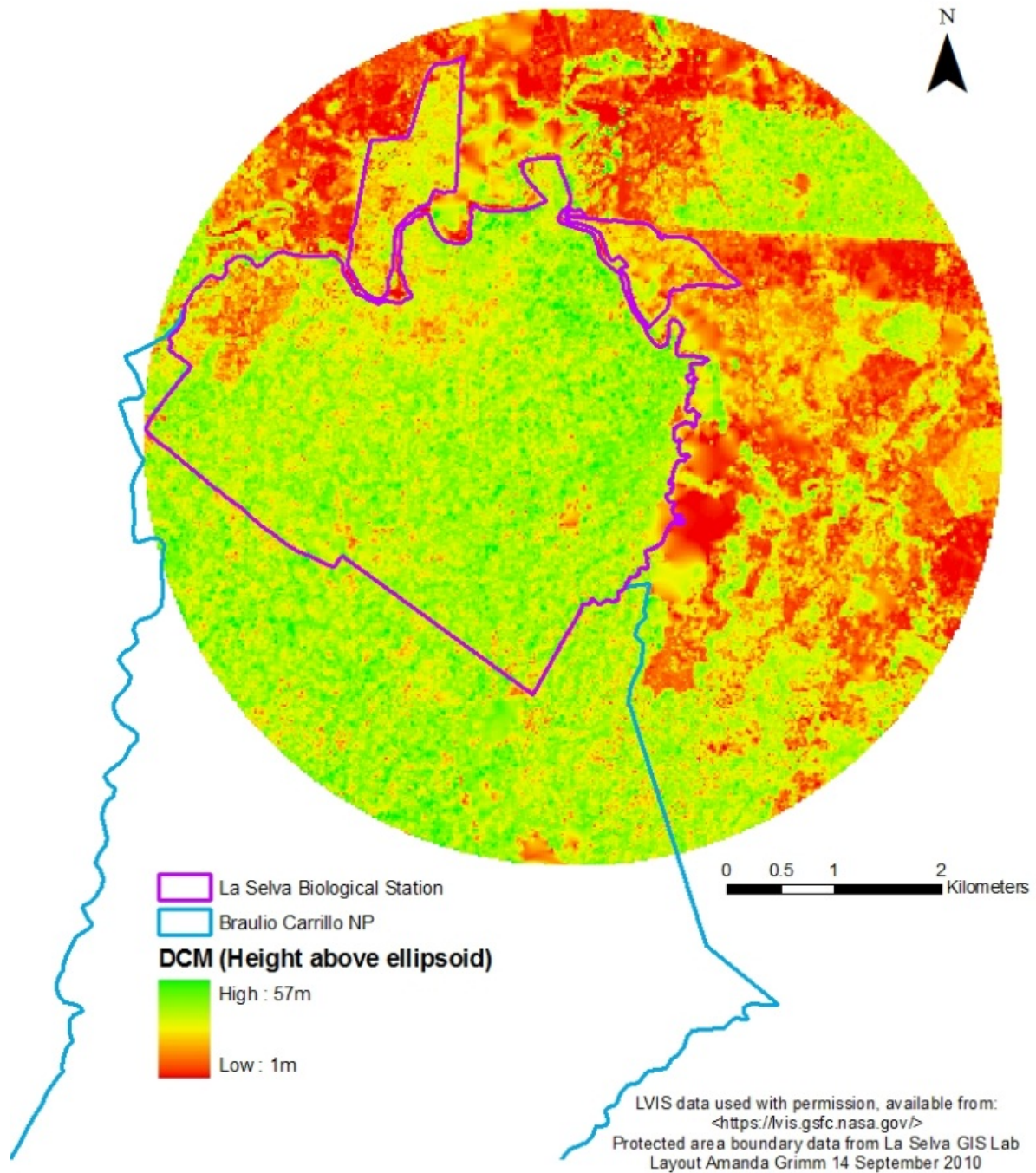
7 CONCLUSIONS

While it was difficult to correlate lidar-generated measures of understory density with field-based measures of biomass and density, lidar metrics significantly improved models of habitat suitability for individual bird species. Metrics derived from lidar are useful for quantifying the multi-dimensional structure of forest habitat at the landscape scale. Habitat models for different species of understory insectivore exhibited some guild-wide similarities as well as important differences. Both habitat patch size and understory condition are likely to factor significantly into habitat suitability for this guild.

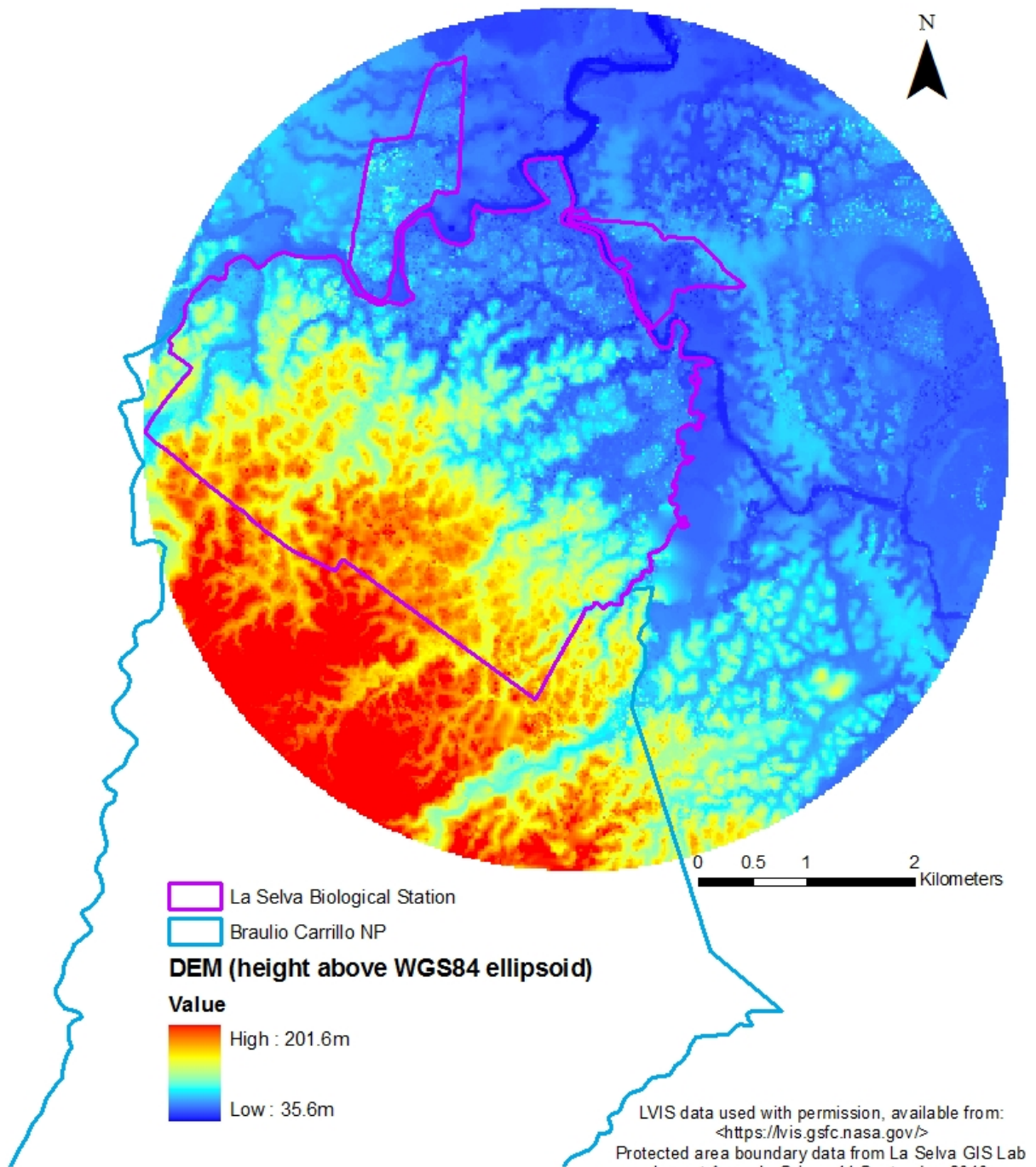
8 APPENDICES

8.1 Appendix 1: Mapped environmental variables used in MaxEnt models.

LVIS 2005 - Canopy Height Estimate

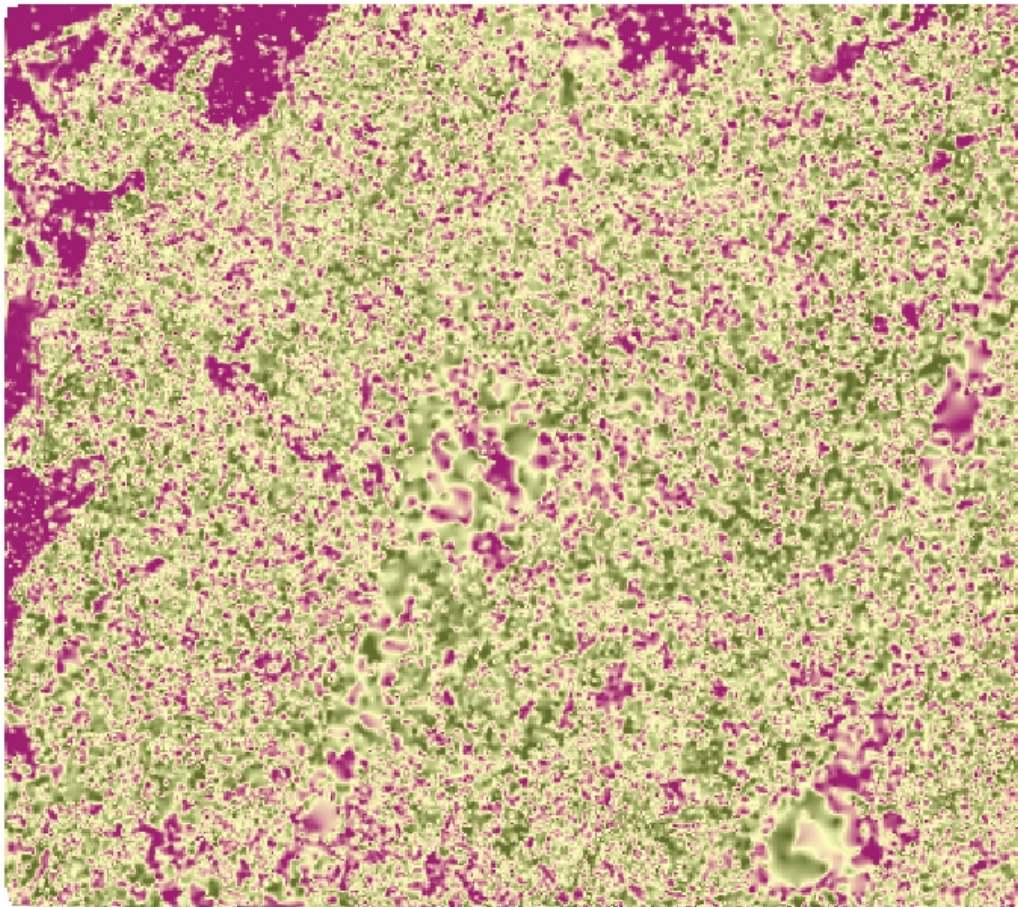


LVIS 2005 - DEM

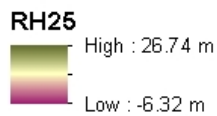


Volcan Barva

LVIS 2005: The Height at Which 25% of the Energy in the Raw Waveform Occurs Relative to the Estimated Elevation



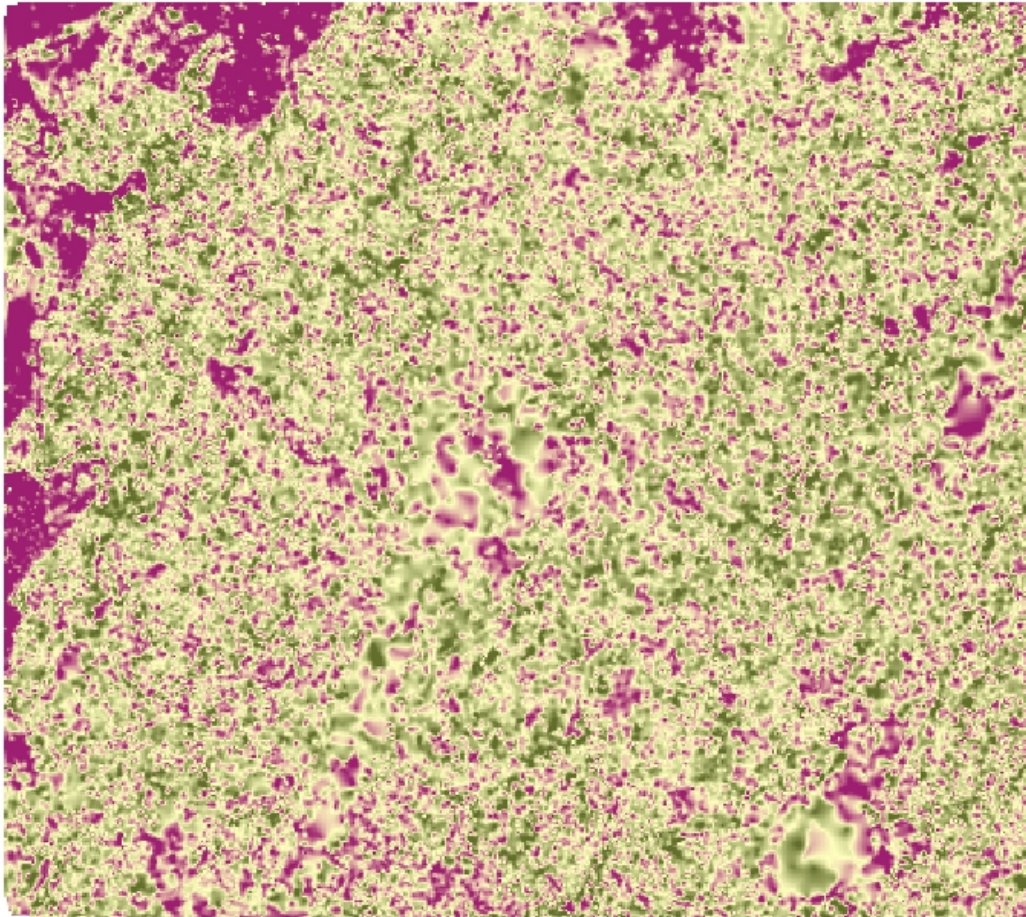
0 500 1,000 2,000 Meters



Raster created from LVIS waveform data provided by Goddard Space Flight Center. Analysis & map design by Amanda Grimm, 2011.

Volcan Barva

LVIS 2005: The Height at Which 30% of the Energy in the Raw Waveform Occurs Relative to the Estimated Elevation



0 500 1,000 2,000 Meters



Legend

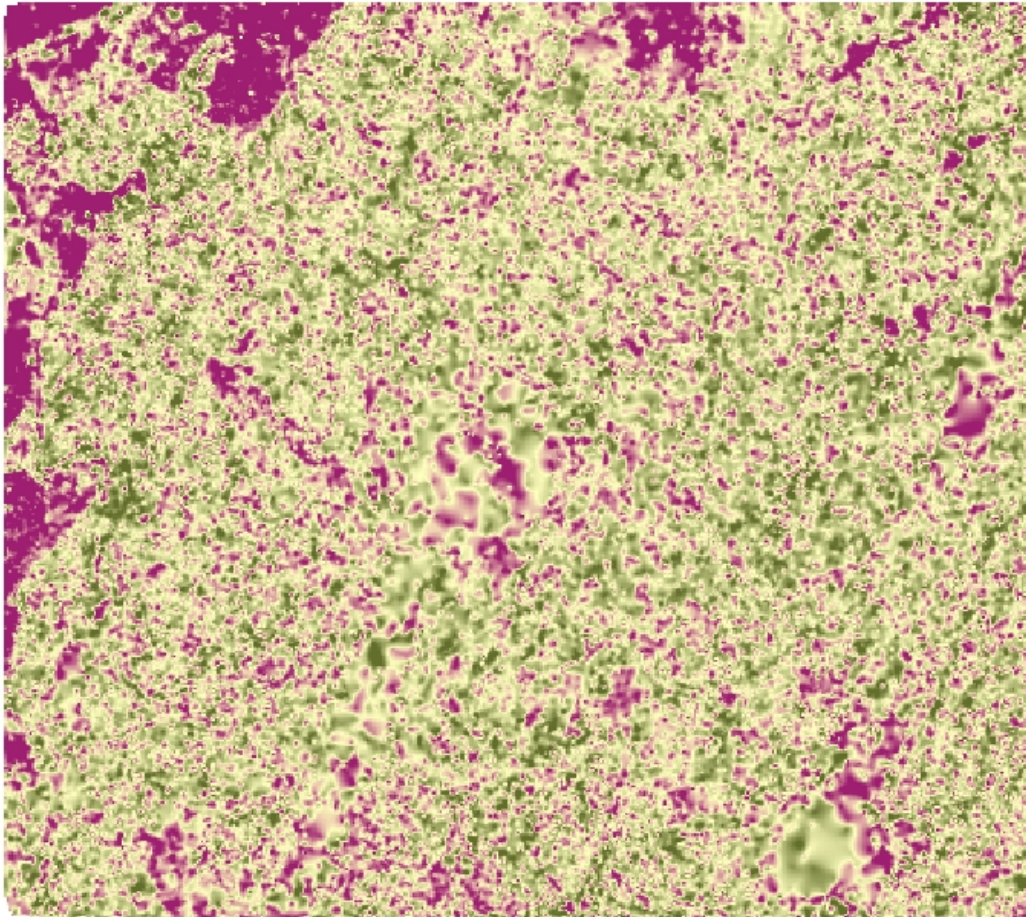
RH30



Raster created from LVIS waveform data provided by Goddard Space Flight Center. Analysis & map design by Amanda Grimm, 2011.

Volcan Barva

LVIS 2005: The Height at Which 40% of the Energy in the Raw Waveform Occurs Relative to the Estimated Elevation



0 500 1,000 2,000 Meters



Legend

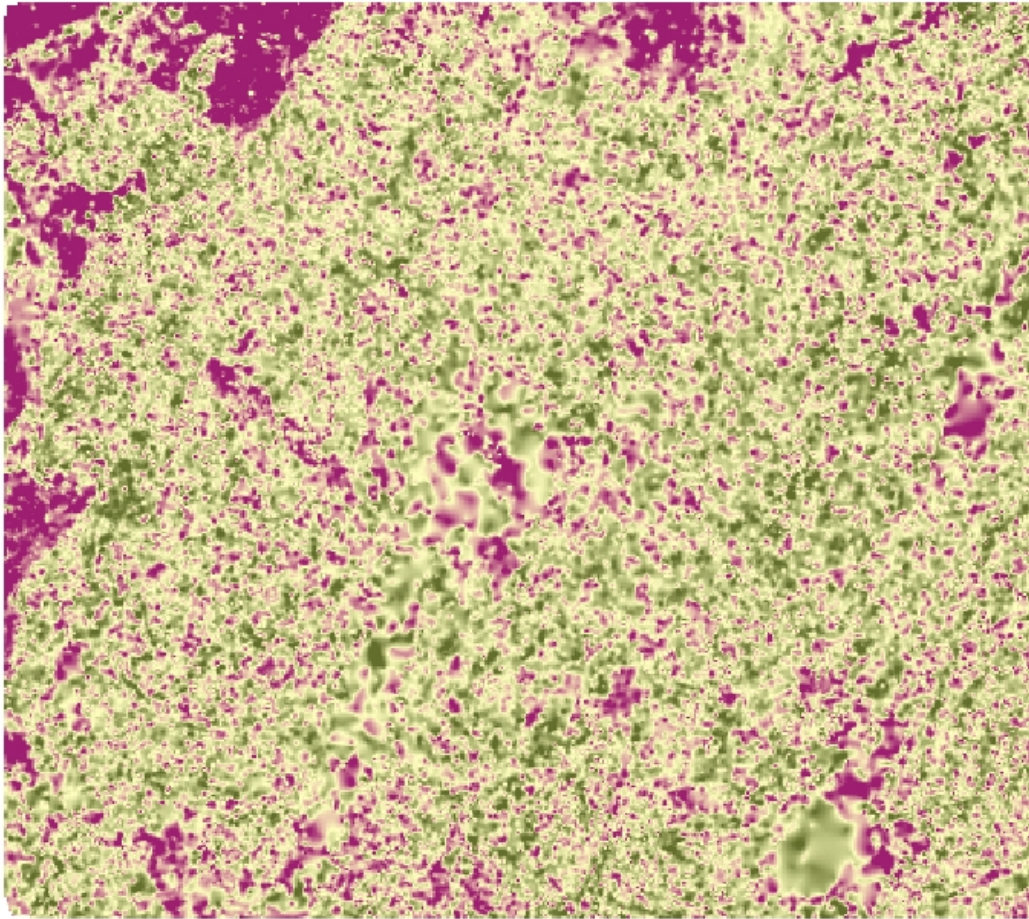
RH40



Raster created from LVIS waveform data provided by Goddard Space Flight Center. Analysis & map design by Amanda Grimm, 2011.

Volcan Barva

LVIS 2005: The Height at Which 50% of the Energy in the Raw Waveform Occurs Relative to the Estimated Elevation



0 500 1,000 2,000 Meters

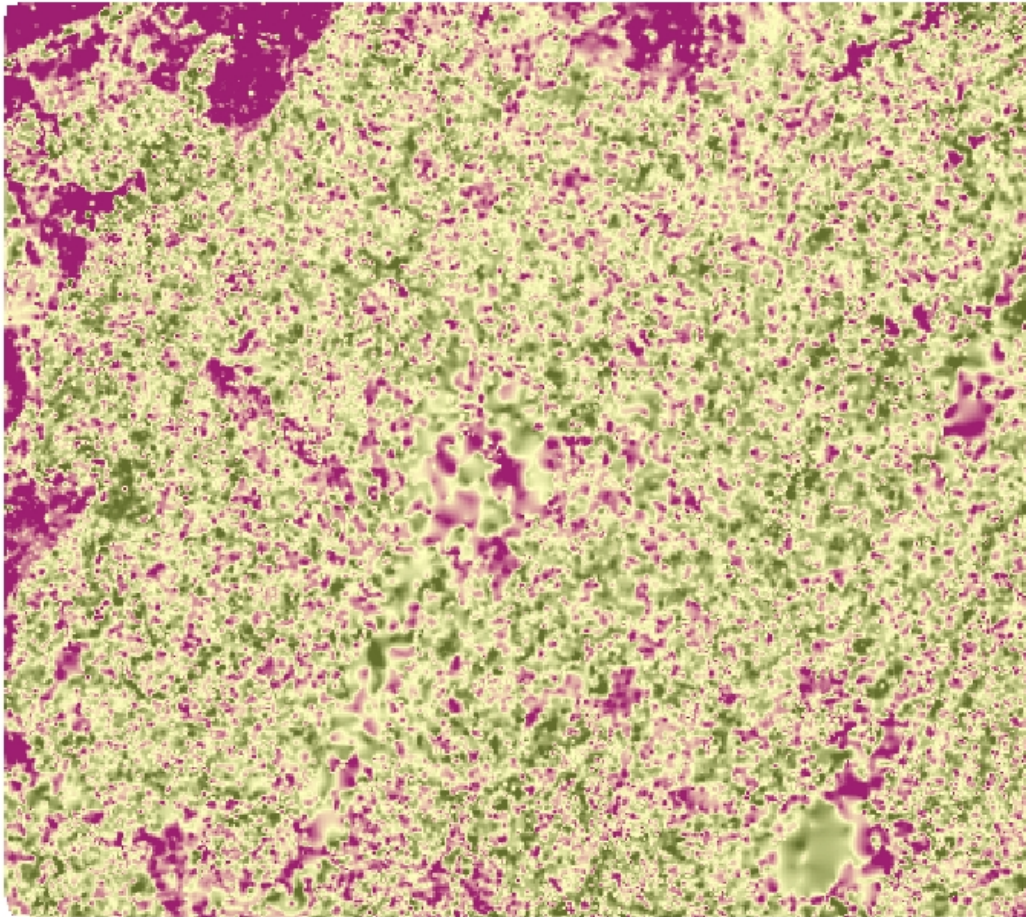


RH50
High : 39.59 m
Low : -2.00 m

Raster created from LVIS waveform data provided by Goddard Space Flight Center. Analysis & map design by Amanda Grimm, 2011.

Volcan Barva

LVIS 2005: The Height at Which 60% of the Energy in the Raw Waveform Occurs Relative to the Estimated Elevation

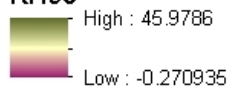


0 500 1,000 2,000 Meters



Legend

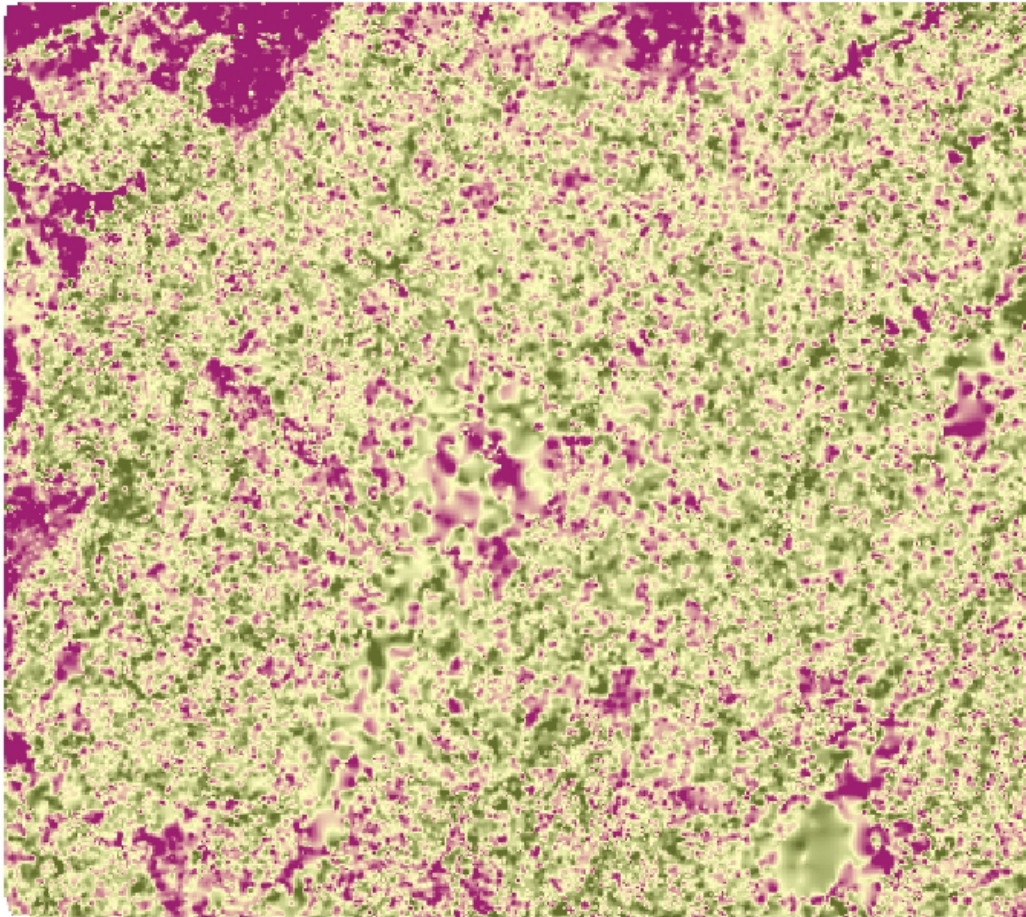
RH60



Raster created from LVIS waveform data provided by Goddard Space Flight Center. Analysis & map design by Amanda Grimm, 2011.

Volcan Barva

LVIS 2005: The Height at Which 70% of the Energy in the Raw Waveform Occurs Relative to the Estimated Elevation

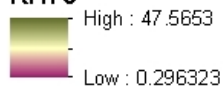


0 500 1,000 2,000 Meters



Legend

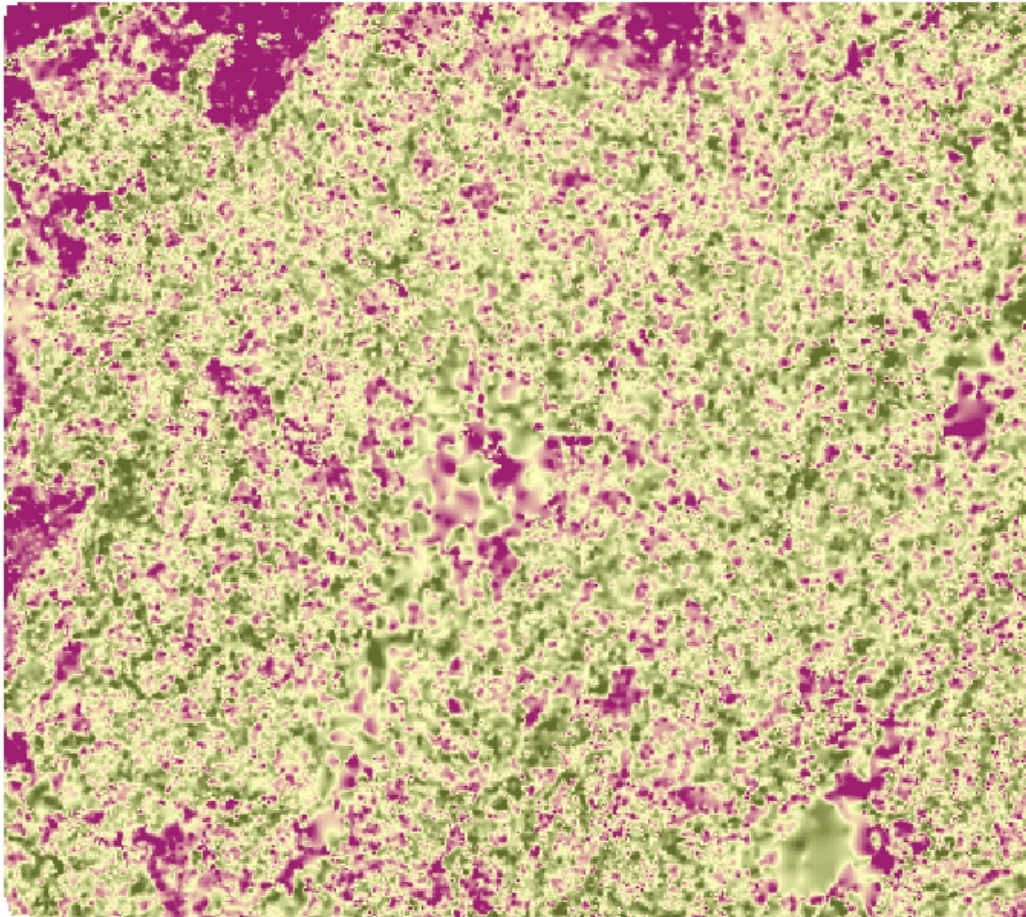
RH70



Raster created from LVIS waveform data provided by Goddard Space Flight Center. Analysis & map design by Amanda Grimm, 2011.

Volcan Barva

LVIS 2005: The Height at Which 75% of the Energy in the Raw Waveform Occurs Relative to the Estimated Elevation



0 500 1,000 2,000 Meters

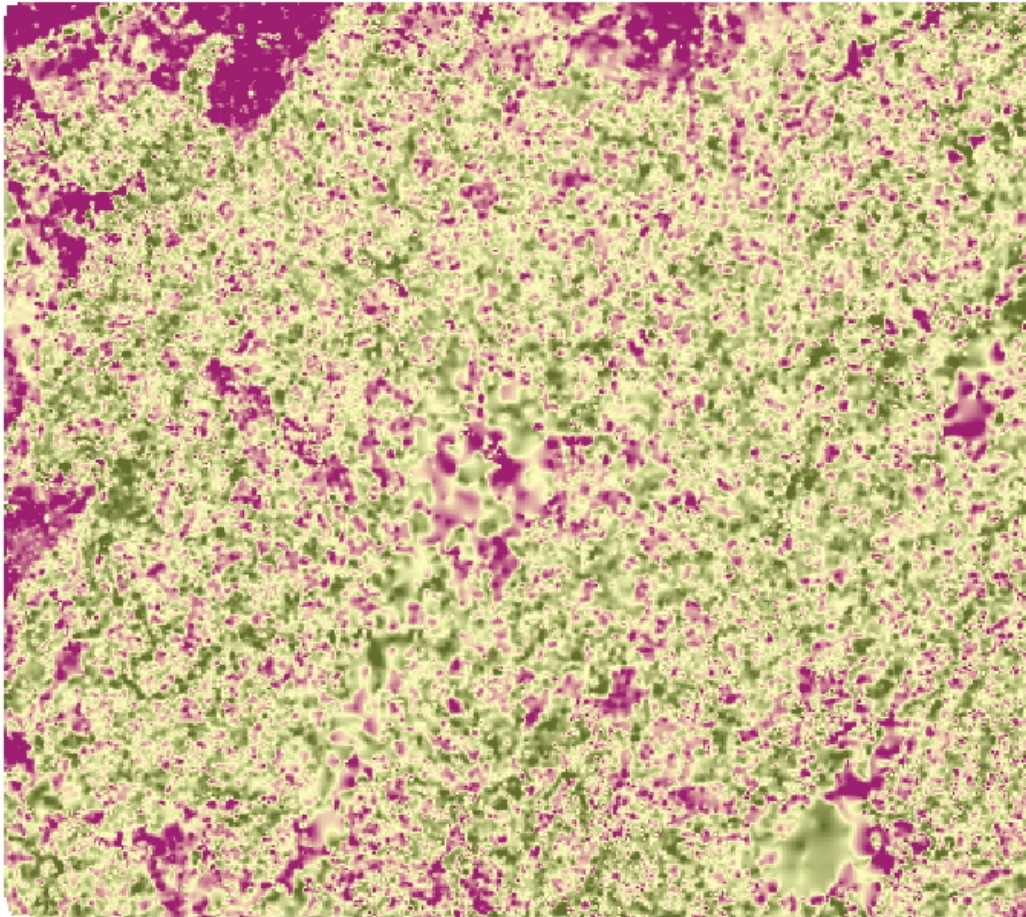


RH75
High : 47.17 m
Low : 0.41 m

Raster created from LVIS waveform data provided by Goddard Space Flight Center. Analysis & map design by Amanda Grimm, 2011.

Volcan Barva

LVIS 2005: The Height at Which 80% of the Energy in the Raw Waveform Occurs Relative to the Estimated Elevation



0 500 1,000 2,000 Meters

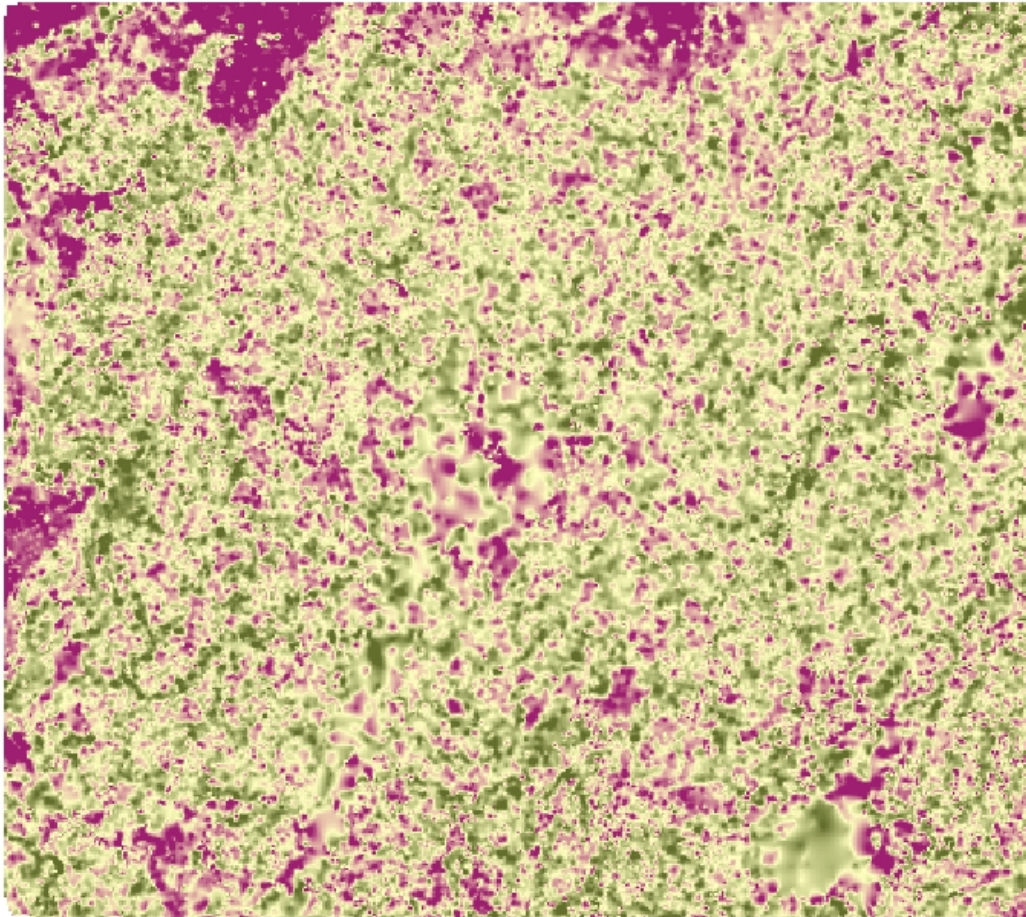


RH80
High : 51.86 m
Low : 0.65 m

Raster created from LVIS waveform data provided by Goddard Space Flight Center. Analysis & map design by Amanda Grimm, 2011.

Volcan Barva

LVIS 2005: The Height at Which 90% of the Energy in the Raw Waveform Occurs Relative to the Estimated Elevation



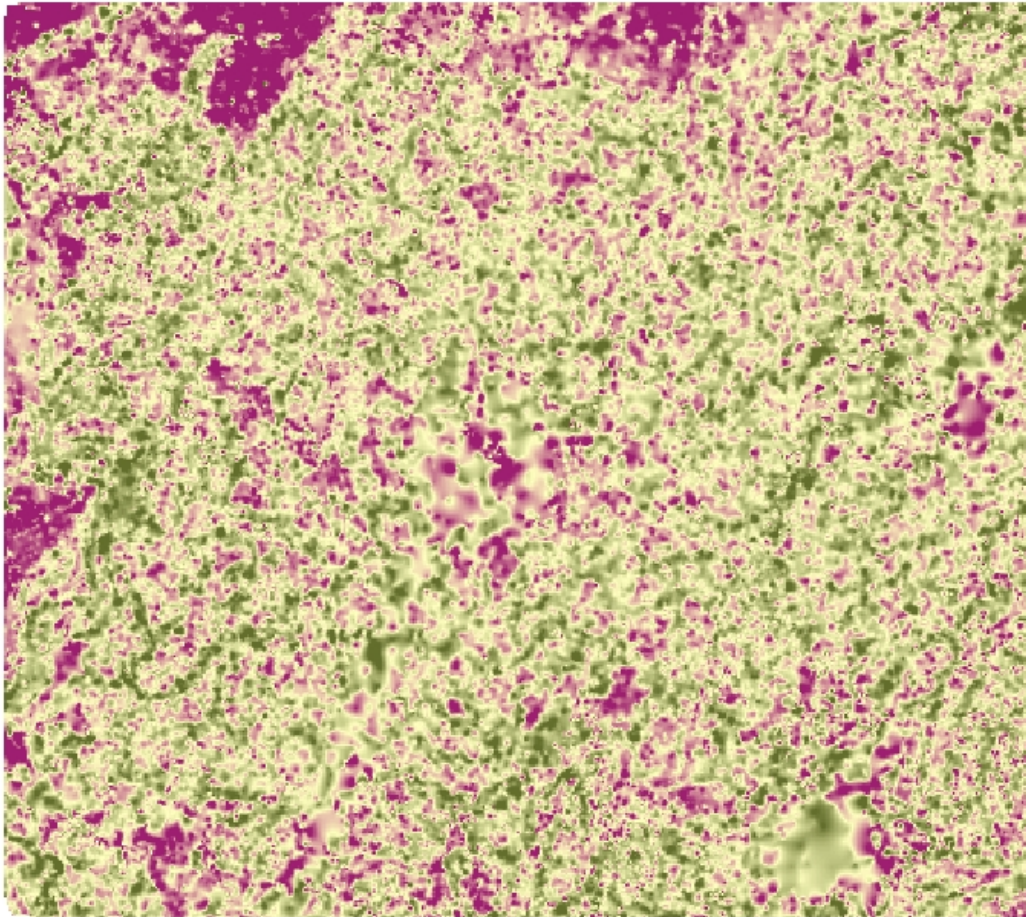
0 500 1,000 2,000 Meters



Raster created from LVIS waveform data provided by Goddard Space Flight Center. Analysis & map design by Amanda Grimm, 2011.

Volcan Barva

LVIS 2005: The Height at Which 95% of the Energy in the Raw Waveform Occurs Relative to the Estimated Elevation



0 500 1,000 2,000 Meters

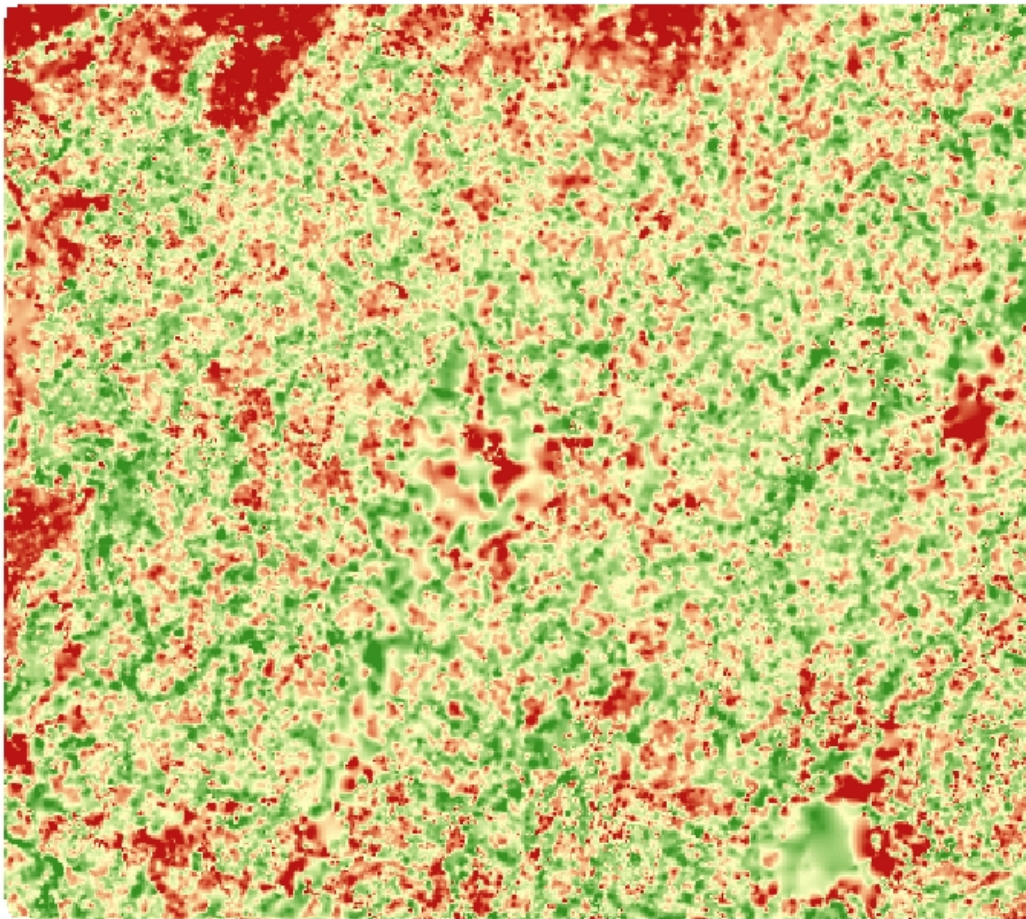


RH95
High : 56.76 m
Low : 1.29 m

Raster created from LVIS waveform data provided by Goddard Space Flight Center. Analysis & map design by Amanda Grimm, 2011.

Volcan Barva

LVIS 2005: Maximum Canopy Height (rh100)



0 500 1,000 2,000 Meters

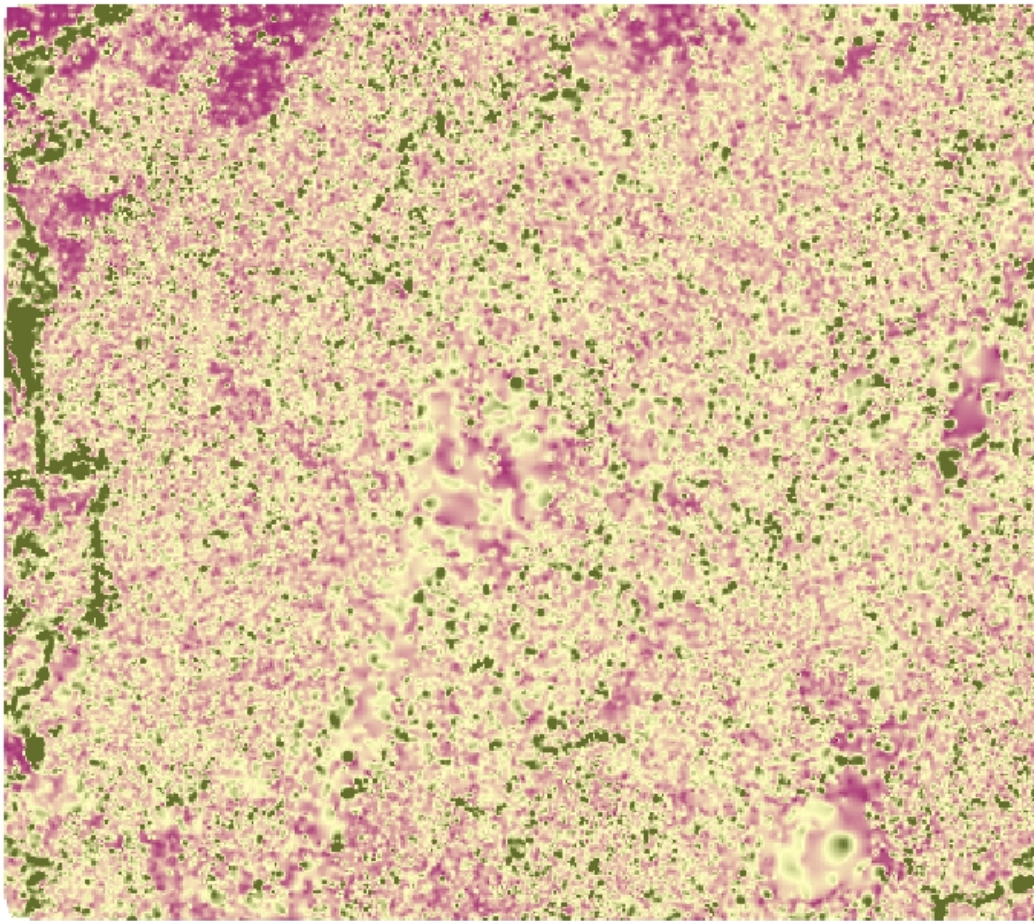


RH100
High : 66.63 m
Low : 1.45 m

Raster created from LVIS waveform data provided by Goddard Space Flight Center. Analysis & map design by Amanda Grimm, 2011.

Volcan Barva

LVIS 2005: Height at Which 10% of the Canopy Height Profile (CHP) Occurs Relative to Estimated Elevation



0 500 1,000 2,000 Meters



CHPRH10

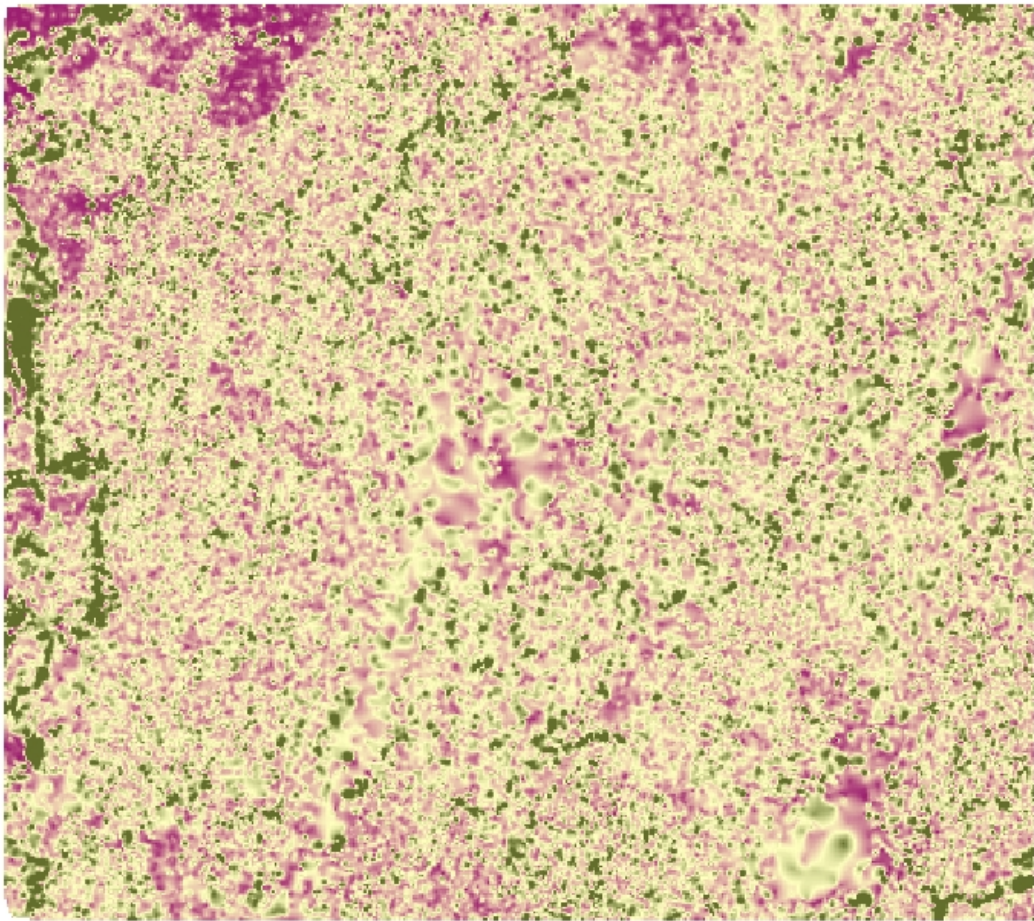
Value

High : 32.1152
Low : 0.0450955

Raster created from LVIS waveform data provided by Goddard Space Flight Center. Analysis & map design by Amanda Grimm, 2011.

Volcan Barva

LVIS 2005: Height at Which 15% of the Canopy Height Profile (CHP) Occurs Relative to Estimated Elevation

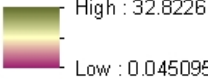


0 500 1,000 2,000 Meters



CHPRH15

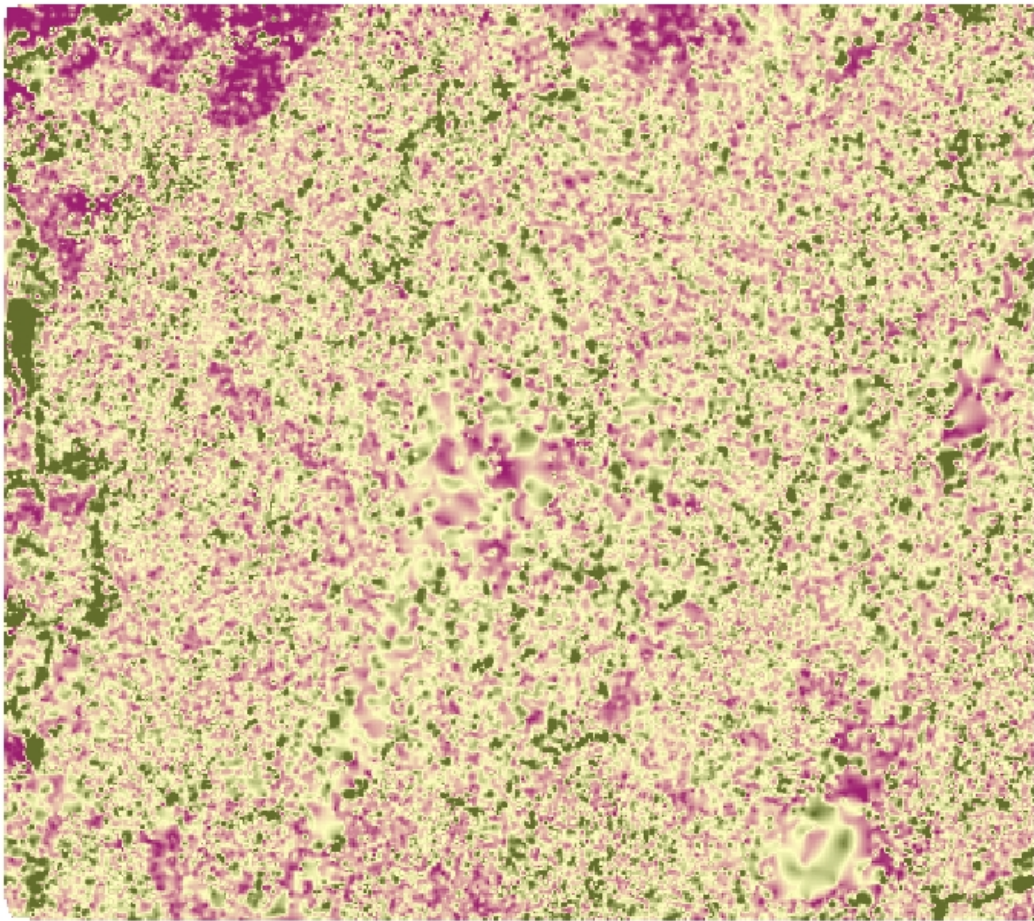
Value



Raster created from LVIS waveform data provided by Goddard Space Flight Center. Analysis & map design by Amanda Grimm, 2011.

Volcan Barva

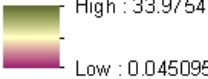
LVIS 2005: Height at Which 20% of the Canopy Height Profile (CHP) Occurs Relative to Estimated Elevation



Legend

CHPRH20

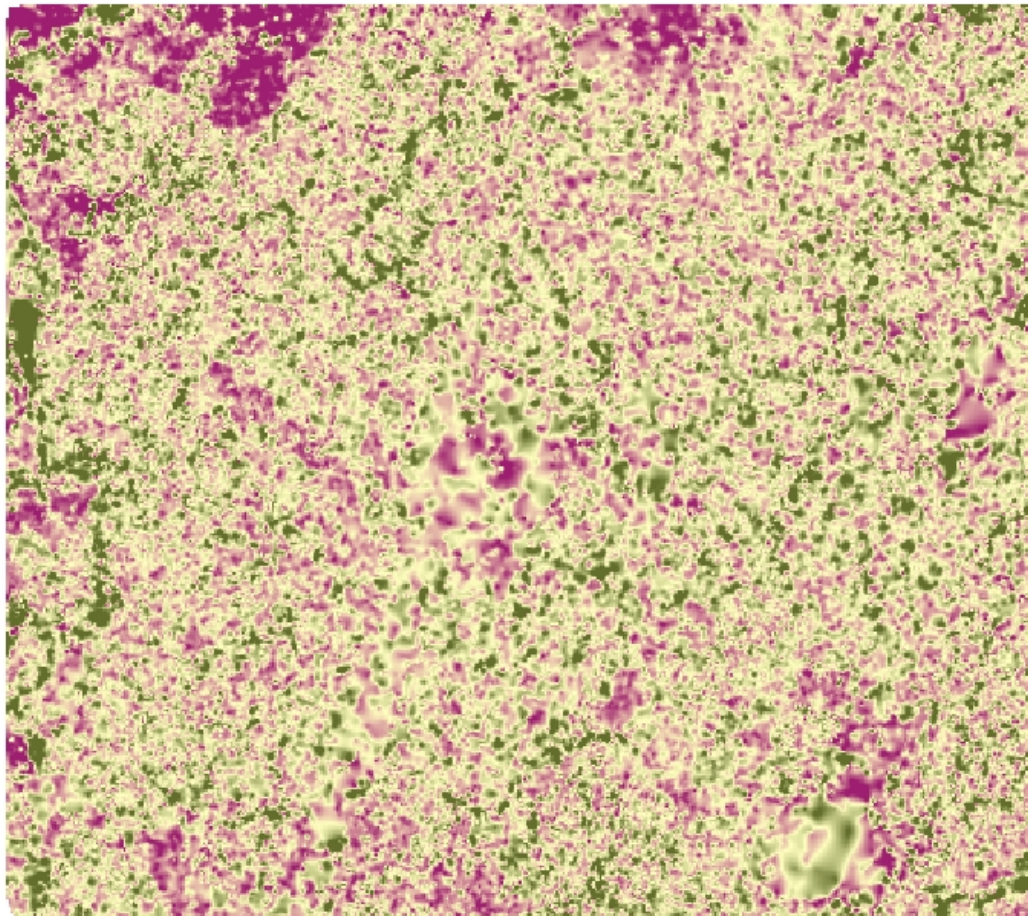
Value



Raster created from LVIS waveform data provided by Goddard Space Flight Center. Analysis & map design by Amanda Grimm, 2011.

Volcan Barva

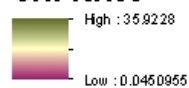
LVIS 2005: Height at Which 30% of the Canopy Height Profile (CHP) Occurs Relative to Estimated Elevation



0 500 1,000 2,000 Meters



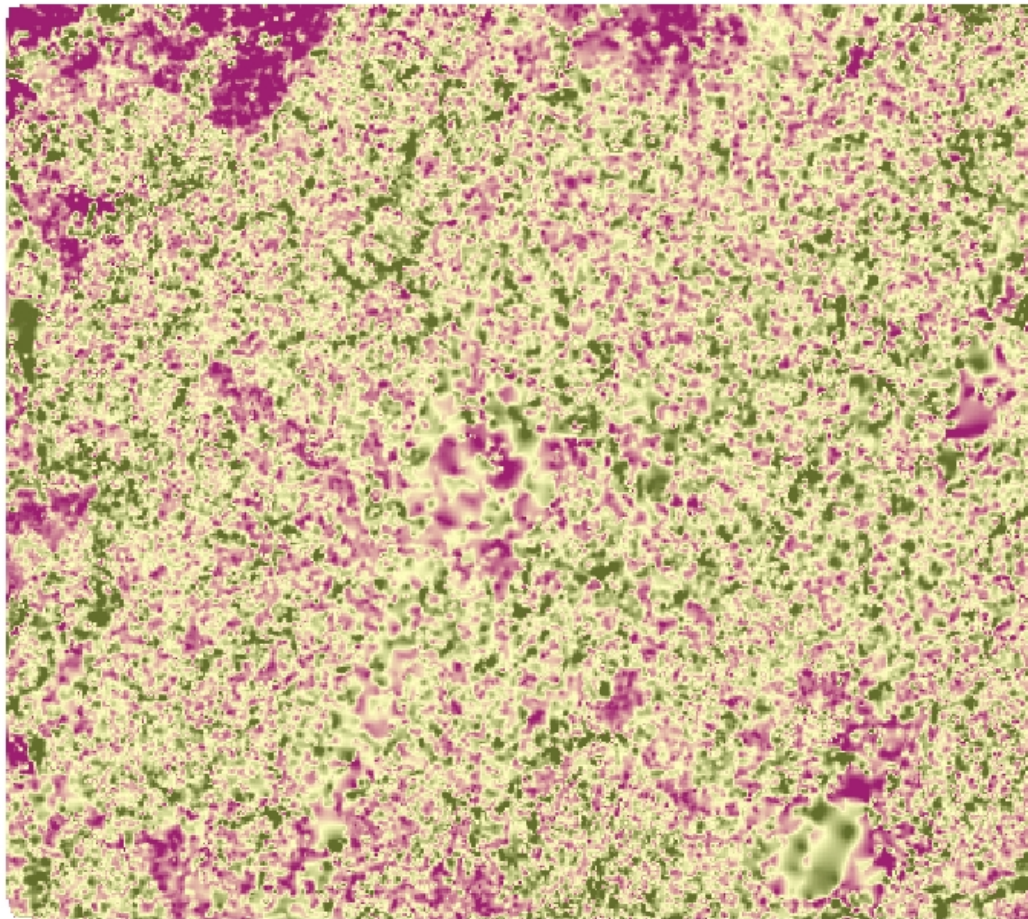
CHPRH30



Raster created from LVIS waveform data provided by Goddard Space Flight Center. Analysis & map design by Amanda Grimm, 2011.

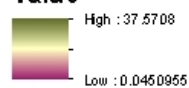
Volcan Barva

LVIS 2005: Height at Which 40% of the Canopy Height Profile (CHP) Occurs Relative to Estimated Elevation



CHPRH40

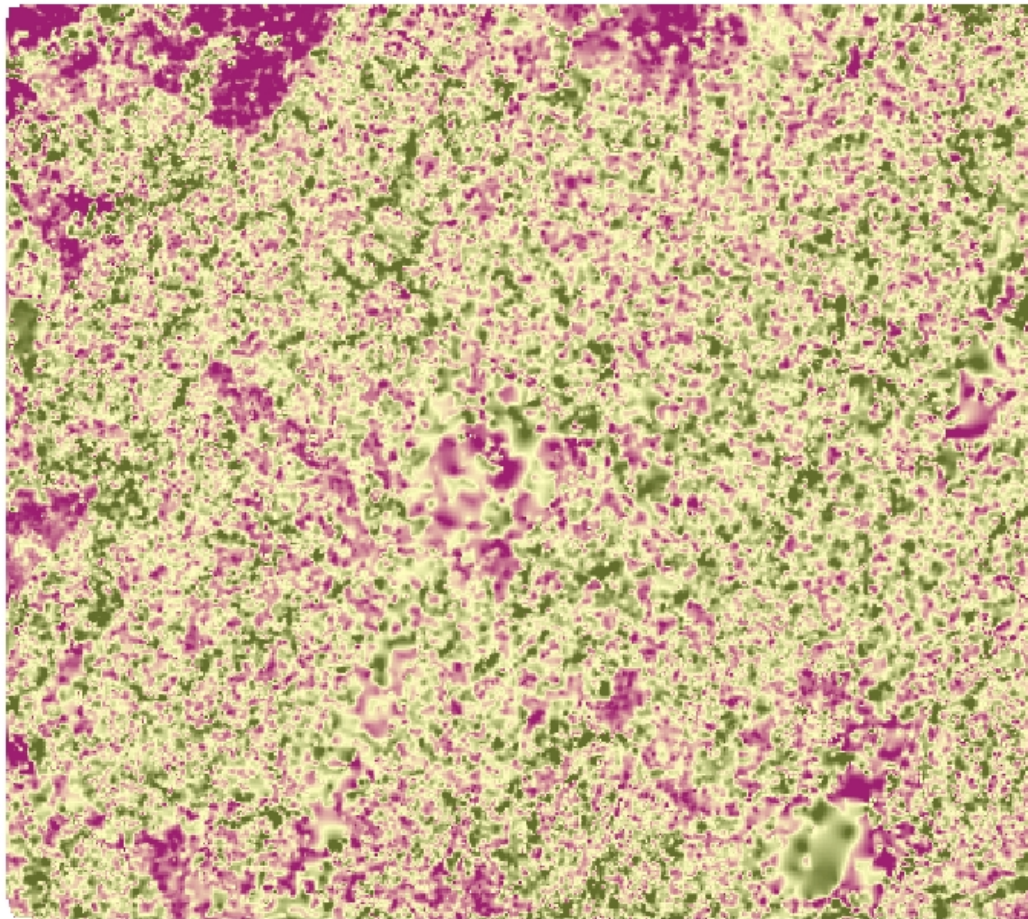
Value



Raster created from LVIS waveform data provided by Goddard Space Flight Center. Analysis & map design by Amanda Grimm, 2011.

Volcan Barva

LVIS 2005: Height at Which 50% of the Canopy Height Profile (CHP) Occurs Relative to Estimated Elevation



CHPRH50

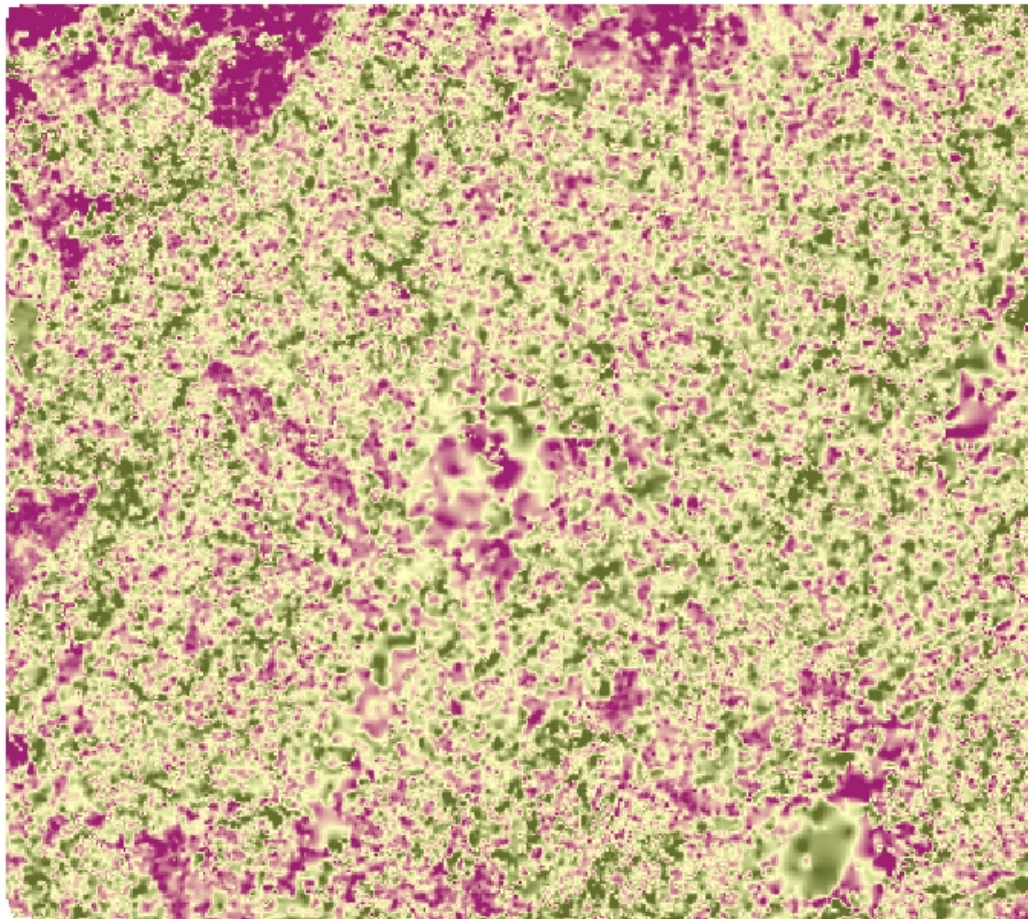
Value



Raster created from LVIS waveform data provided by Goddard Space Flight Center. Analysis & map design by Amanda Grimm, 2011.

Volcan Barva

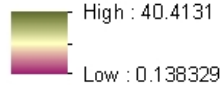
LVIS 2005: Height at Which 60% of the Canopy Height Profile (CHP) Occurs Relative to Estimated Elevation



Legend

CHPRH60

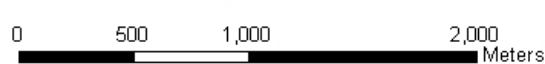
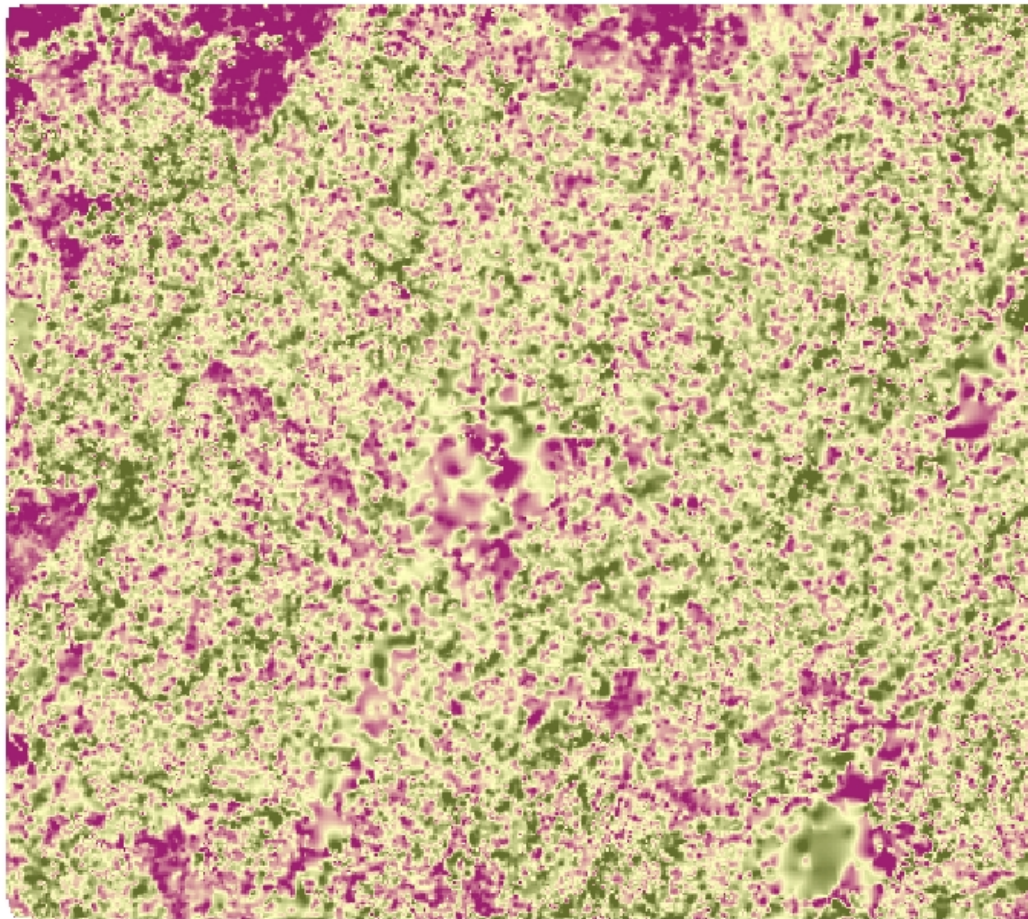
Value



Raster created from LVIS waveform data provided by Goddard Space Flight Center. Analysis & map design by Amanda Grimm, 2011.

Volcan Barva

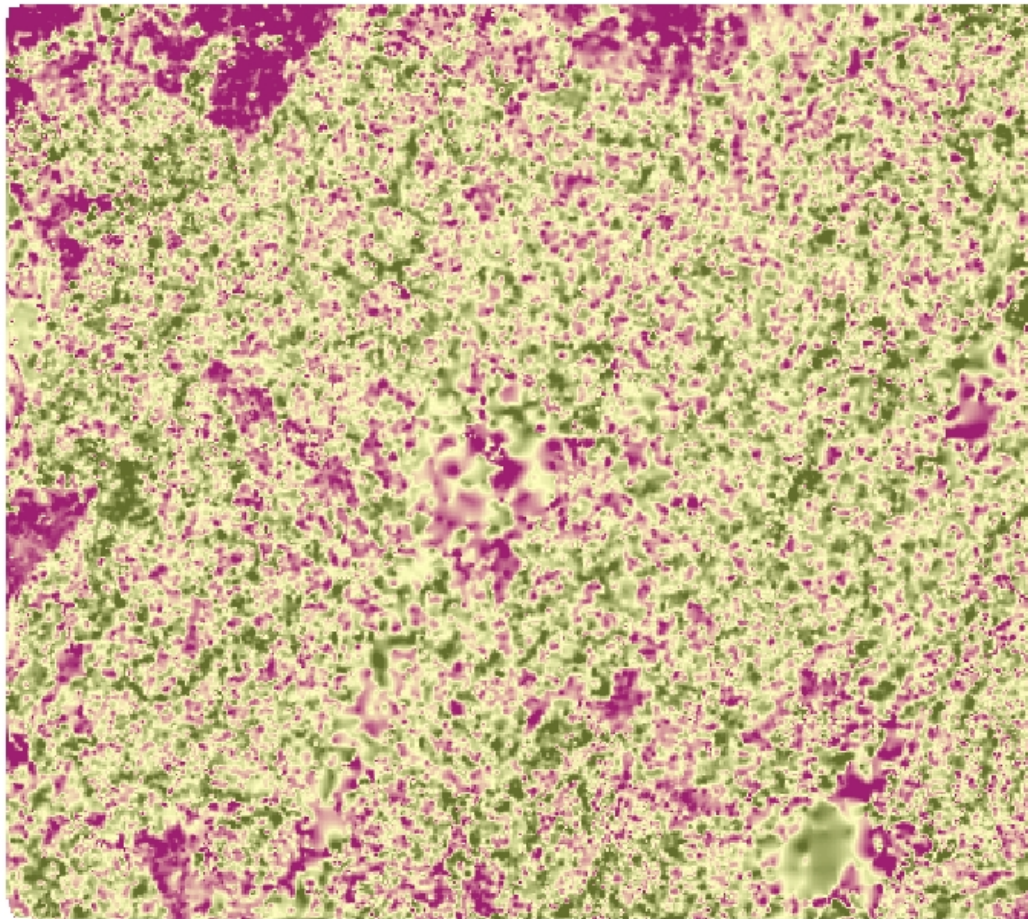
LVIS 2005: Height at Which 70% of the Canopy Height Profile (CHP) Occurs Relative to Estimated Elevation



Raster created from LVIS waveform data provided by Goddard Space Flight Center. Analysis & map design by Amanda Grimm, 2011.

Volcan Barva

LVIS 2005: Height at Which 80% of the Canopy Height Profile (CHP) Occurs Relative to Estimated Elevation



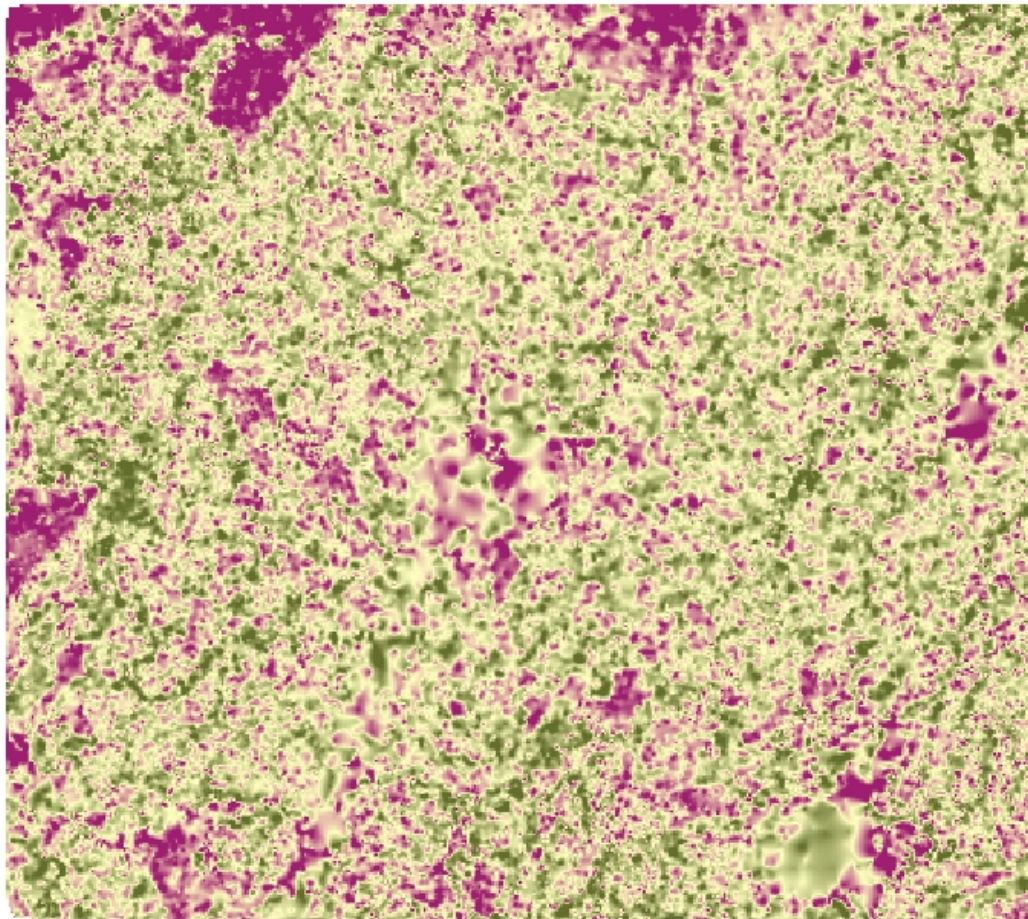
0 500 1,000 2,000 Meters



Raster created from LVIS waveform data provided by Goddard Space Flight Center. Analysis & map design by Amanda Grimm, 2011.

Volcan Barva

LVIS 2005: Height at Which 90% of the Canopy Height Profile (CHP) Occurs Relative to Estimated Elevation



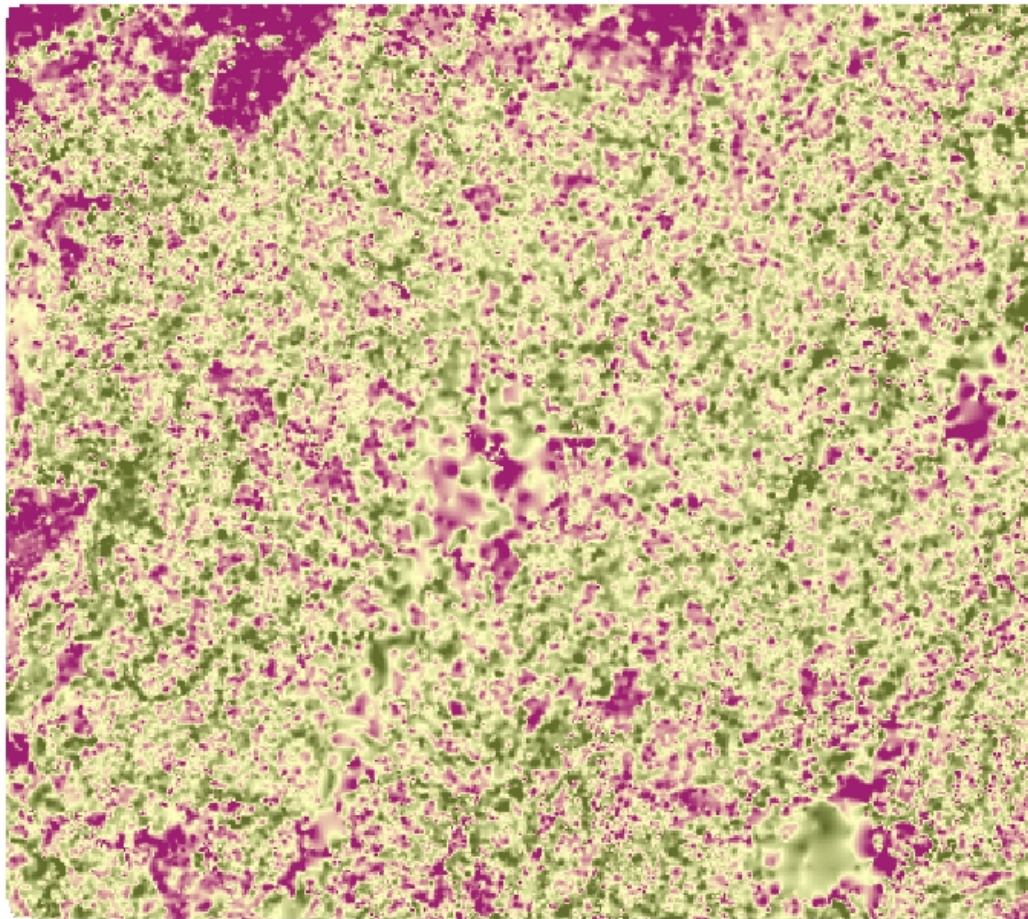
0 500 1,000 2,000 Meters



Raster created from LVIS waveform data provided by Goddard Space Flight Center. Analysis & map design by Amanda Grimm, 2011.

Volcan Barva

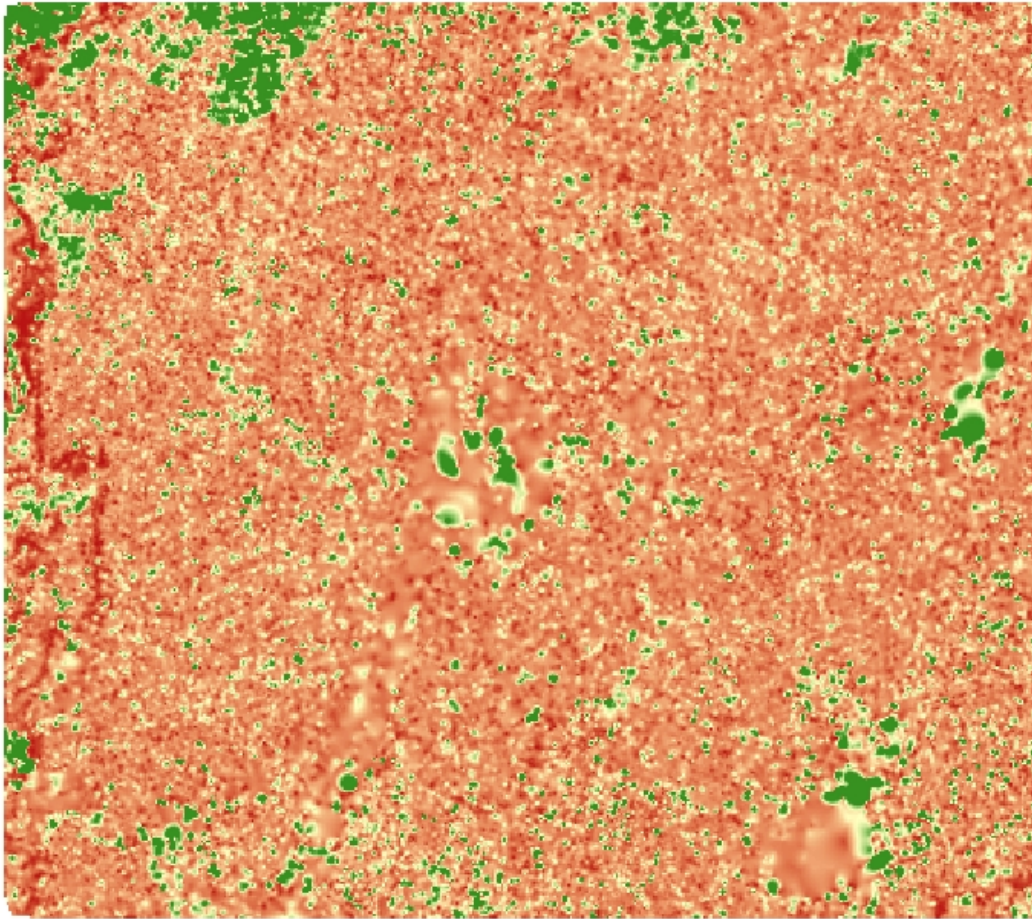
LVIS 2005: Height at Which 95% of the Canopy Height Profile (CHP) Occurs Relative to Estimated Elevation



Raster created from LVIS waveform data provided by Goddard Space Flight Center. Analysis & map design by Amanda Grimm, 2011.

Volcan Barva

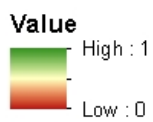
LVIS 2005: Proportion of the Canopy Height Profile (CHP) Occurring from 0-1.5 m Above the Ground



0 500 1,000 2,000 Meters



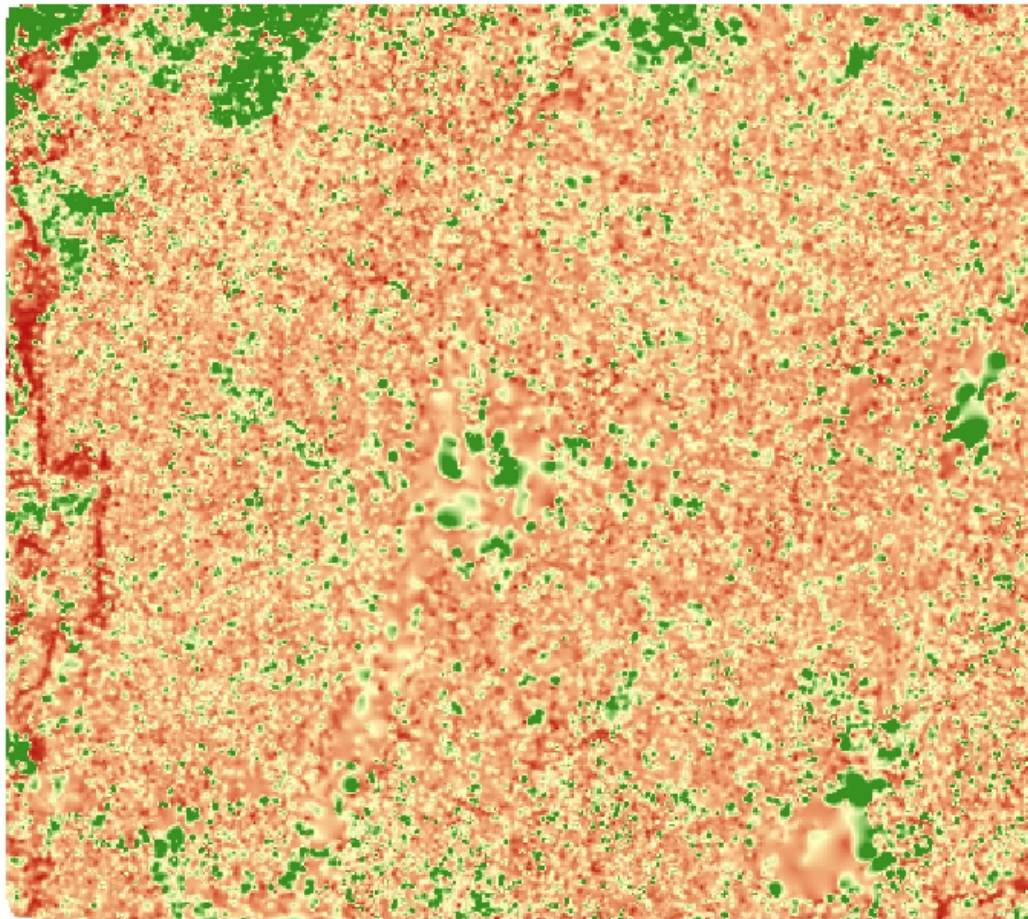
CHP 0-1.5



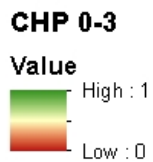
Raster created from LVIS waveform data provided by Goddard Space Flight Center. Analysis & map design by Amanda Grimm, 2011.

Volcan Barva

LVIS 2005: Proportion of the Canopy Height Profile (CHP) Occurring from 0-3 m Above the Ground



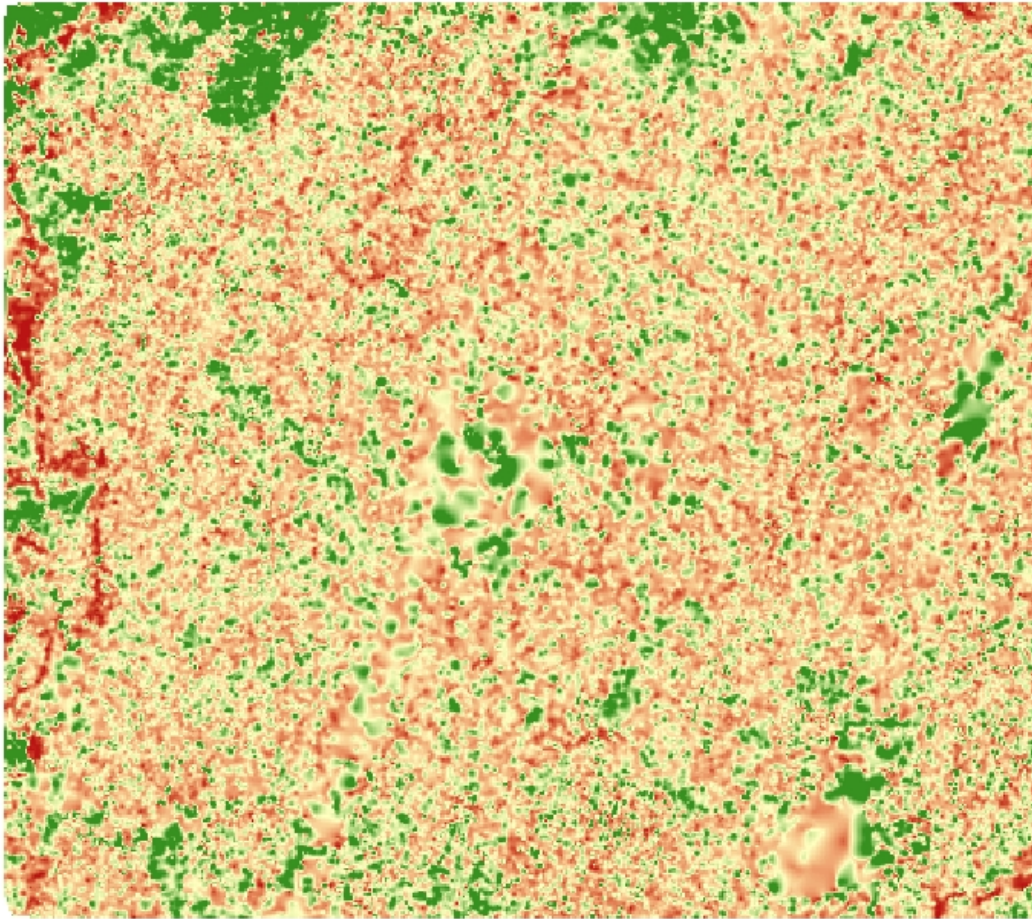
0 500 1,000 2,000 Meters



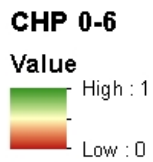
Raster created from LVIS waveform data provided by Goddard Space Flight Center. Analysis & map design by Amanda Grimm, 2011.

Volcan Barva

LVIS 2005: Proportion of the Canopy Height Profile (CHP) Occurring from 0-6 m Above the Ground



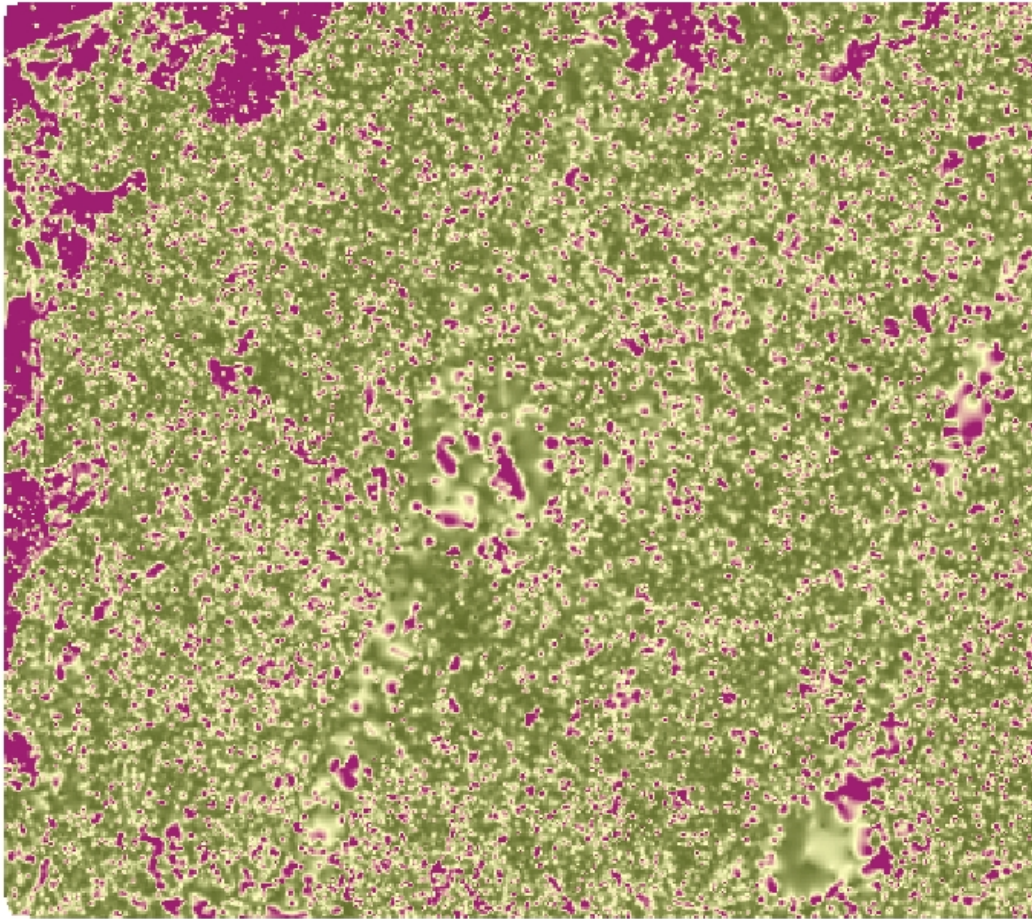
0 500 1,000 2,000 Meters



Raster created from LVIS waveform data provided by Goddard Space Flight Center. Analysis & map design by Amanda Grimm, 2011.

Volcan Barva

LVIS 2005: Percent Canopy Cover



0 500 1,000 2,000 Meters

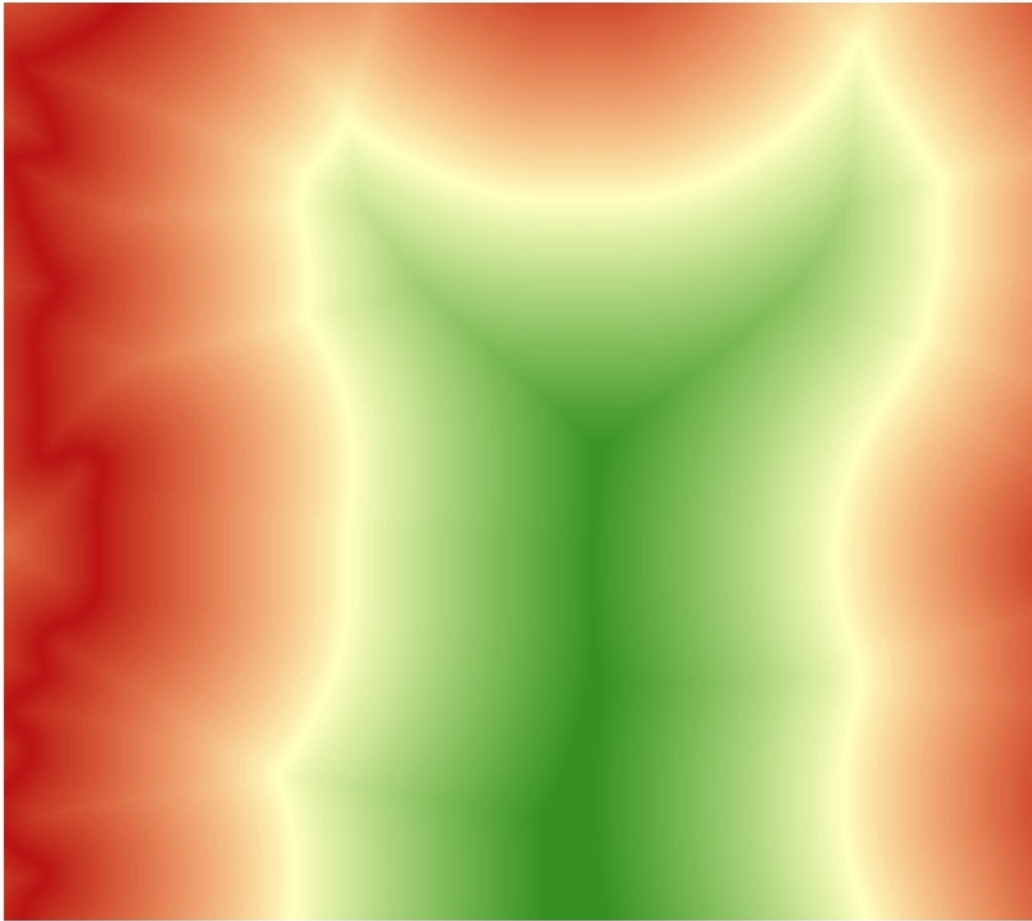


Percent Cover
High : 0.998252
Low : 0.000497269

Raster created from LVIS waveform data provided by Goddard Space Flight Center. Analysis & map design by Amanda Grimm, 2011.

Volcan Barva

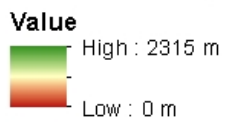
LVIS 2005: Distance to Forest Edge



0 500 1,000 2,000 Meters



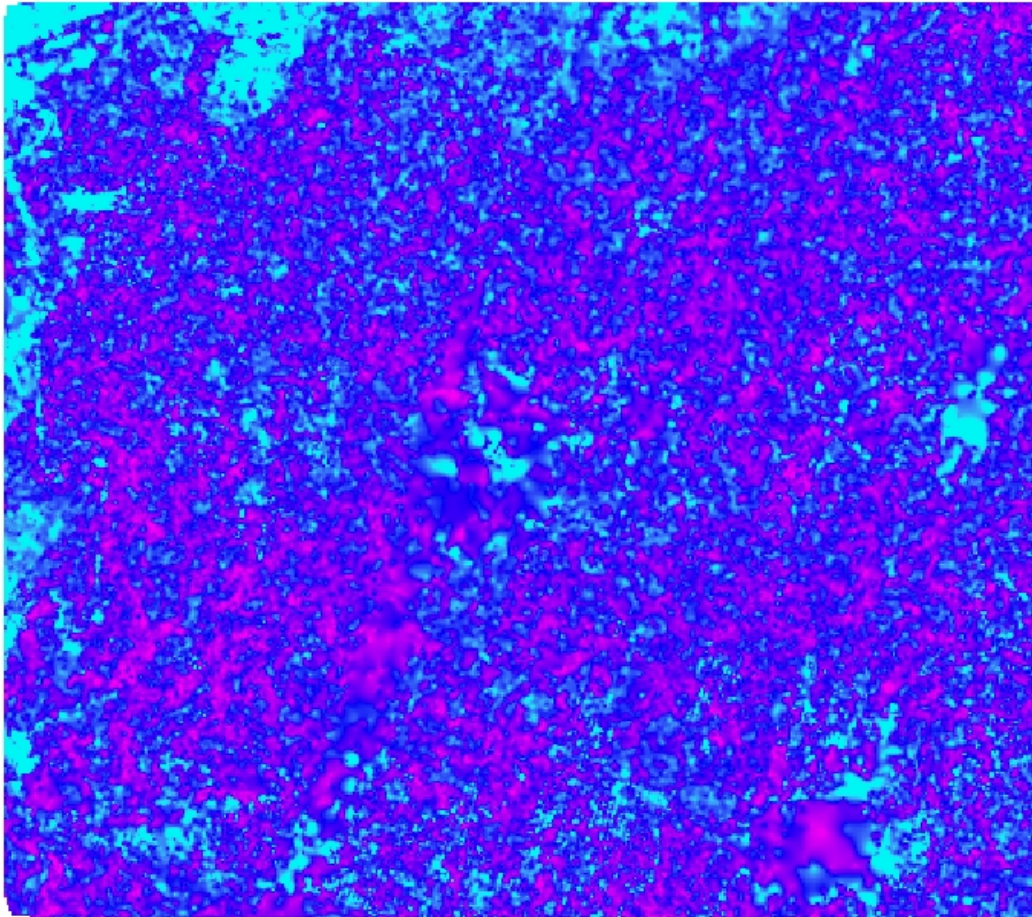
Distance to Edge



Raster created from LVIS waveform data provided by Goddard Space Flight Center. Analysis & map design by Amanda Grimm, 2011.

Volcan Barva

LVIS 2005: Foliage Height Diversity



0 500 1,000 2,000
Meters



Legend

FHD

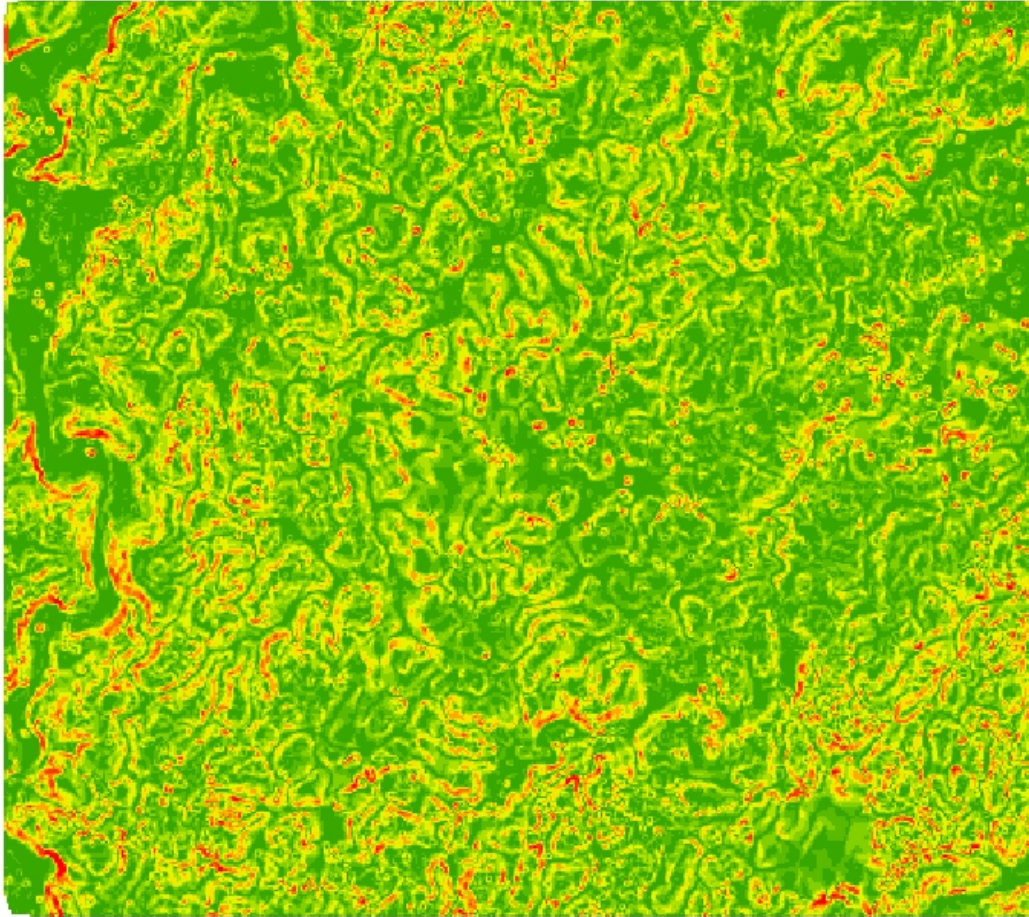


High : 5.12448

Low : 1.90479











Raster created from LVIS waveform data provided by Goddard Space Flight Center. Analysis & map design by Amanda Grimm, 2011.

Volcan Barva Slope (Percent Rise)



0 500 1,000 2,000 Meters

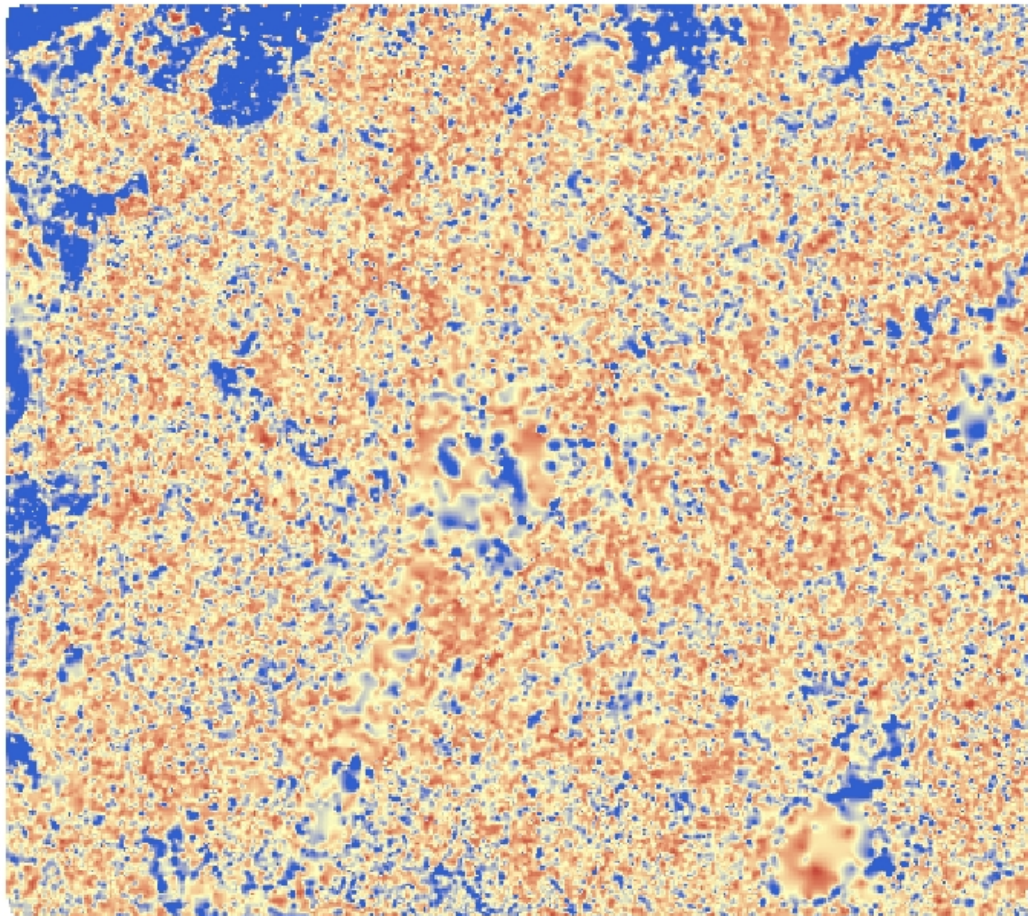


Percent Slope		
 <15	 35 - 45	 80 - 95
 15 - 25	 45 - 55	 95 - 120
 25 - 35	 55 - 65	 >120
	 65 - 80	

Percent slope for portions of La Selva Biological Station an Braulio Carrillo National Park. Created from a DEM of the area based on LVIS large-footprint lidar data collected int 2005. Cell size 10x10m. Lidar data used with permission from Goddard Space Flight Center. Analysis & map design by Amanda Grimm, 2011.

Volcan Barva

LVIS 2005: Vertical Distribution Ratio (VDR)

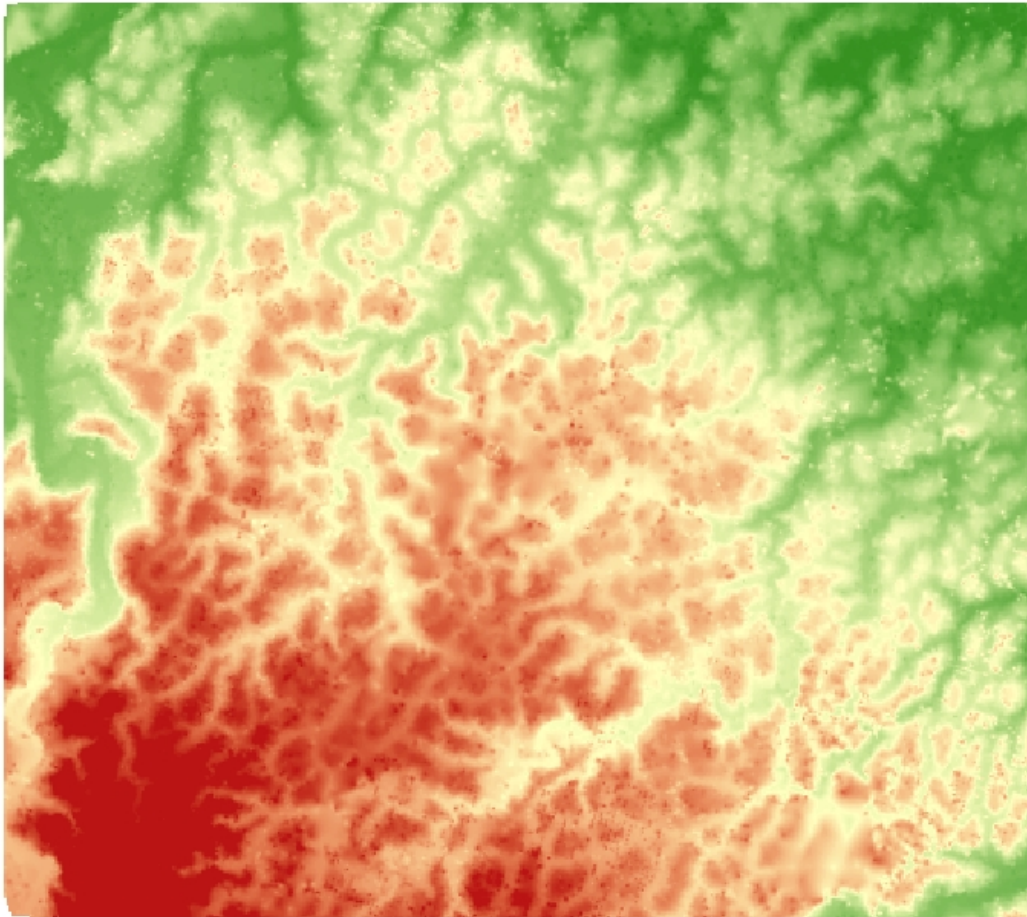


0 500 1,000 2,000 Meters



Raster created from LVIS waveform data provided by Goddard Space Flight Center. Analysis & map design by Amanda Grimm, 2011.

Volcan Barva Elevation (Height Above WGS-84 Ellipsoid)



0 500 1,000 2,000 Meters



Elevation



High : 220.2 m

Low : 37.7 m

Elevation for portions of La Selva Biological Station an Braulio Carrillo National Park. Created from LMS large-footprint lidar data collected in 2005. Cell size 10x10m. Lidar data used with permission from Goddard Space Flight Center. Analysis & map design by Amanda Grimm, 2011.

8.2 Appendix 2: Growth forms and adult statures of La Selva tree species, used for parameterizing fractal models.

Genus	Species	Count in Plots	Growth form (Tall, Midstory, Understory, Palm)	Adult stature (m)	Source
Alchorneopsis	floribunda	7	T	?	Grandtner 2004
Anaxagorea	crassipetala	21	U	10	Armstrong and Marsh 1997
Annona	montana	1	M	15	Contributions from the United States National Herbarium, Volume 18
Apeiba	membranacea	7	T	30	Gargiullo 2008
Apeiba	membranacea	2	T	30	Gargiullo 2008
Astrocaryum	confertum	1	P	15	Shumway 2009
Balizia	elegans	1	T	22	Puig 2005
Borojoa	panamensis	1	M	?	Grandtner 2004
Brosimum	guianensis	1	T	40	The Wood Explorer Database
Brosimum	lactescens	20	T	30	Miranda 2004
Byrsonima	crispa	2	T	25	Weissenhofer 2005
Calophyllum	brasiliense	2	T	45	Lugo and Alayon 2003
Capparis	pittieri	5	U	?	Finegan et al. 1999
Casearia	arborea	34	M	20	Croat 1978
Casearia	commersoniana	1	U	10	Herbarium of the Smithsonian Tropical Research Institute
Casearia	sylvestris	1	U	7	Allen 1977
Cassipourea	elliptica	1	T	25	Herbarium of the Smithsonian Tropical Research Institute
Cecropia	insignis	3	T	30	Brokaw 1999
Cecropia	obtusifolia	2	M	20	Gargiullo 2008
Cedrela	odorata	2	T	40	Gargiullo 2008
Chrysophyllum	venezuelanense	1	T	?	Grandtner 2004
Clarisia	mexicana	2	T	30	Allen 1977
Colubrina	spinosa	2	U	7	Flora of Costa Rica
Compsoeura	mexicana	1	T	30	Janovec and Harrison 2002
Conceveiba	pleiostemona	6	T	?	Grandtner 2004
Cordia	lucidula	1	U	6	Choat et al. 2007
Coussarea	hondensis	3	U	10	Grandtner 2004
Dendropanax	arboreus	27	T	25	Figuroa-Esquivel et al. 2009
Dussia	macrophyllata	7	T	40	Banco de Arboles
Dystovomita	paniculata	2	M	?	Grandtner 2004
Dystovomita	pittieri	1	M	?	Grandtner 2004
Elaeoluma	glabrescens	2	T	?	Grandtner 2004
Eschweilera	longirachis	2	T	?	Grandtner 2004
Eugenia	basilaris	1	U	?	Grandtner 2004
Euterpe	precatória	32	P	25	Shumway 2009

Faramea	glandulosa	5	U	6	Nieder 2001
Faramea	parvibractea	15	M	?	Grandtner 2004
Garcinia	intermedia	1	L	?	Grandtner 2004
Goethalsia	meiantha	15	T	30	Gargiullo 2008
Guarea	bullata	11	T	?	Grandtner 2004
Guarea	guidonia	5	M	20	BRIT Virtual Herbarium
Guarea	hoffmanniana	1	M	15	Allen 1977
Guarea	rhopalocarpa	15	M	20	Gargiullo 2008
Guarea	tuerckheimii	9	T	?	Grandtner 2004
Guatteria	aeruginosa	7	M	15	Allen 1977
Guatteria	diospyroides	1	M	8	Herbarium of the Smithsonian Tropical Research Institute.
Heisteria	concinna	1	M	20	Croat 1978
Hernandia	didymantha	9	T	30	Allen 1977
Hernandia	didymantha	1	T	30	Allen 1977
Hirtella	lemsii	1	M	?	Grandtner 2004
Hirtella	media	1	M	15	Standley 1943
Hyeronima	alchorneoides	1	T	50	Flores 1992
Inga	alba	10	T	23	BRIT Virtual Herbarium
Inga	cocleensis	3	M	13	Croat 1978
Inga	leiocalycina	4	M	?	Bongers 2001
Inga	pezizifera	3	T	27	Croat 1978
Inga	sapindoides	2	M	15	Croat 1978
Inga	thibaudiana	3	U	8	Croat 1978
Inga	umbellifera	3	U	10	Croat 1978
Iriartea	deltoidea	79	P	30	Shumway 2009
Jacaranda	copaia	2	T	30	Herbarium of the Smithsonian Tropical Research Institute
Lacmellea	panamensis	5	M	20	Allen 1977
Lacunaria	panamensis	2	M	15	Flora of Panama
Laetia	procera	8	T	27	King et al. 2006
Licania	affinis	2	M	20	McDade 1994
Licaria	sarapiquensis	2	M	20	Hammel 1986
Maquira	costaricana	1	M	20	Croat 1978
Maranthes	panamensis	2	T	35	Holdridge 2004
Miconia	punctata	1	T	23	(Sawyer and Lindsey 1971)
Minquartia	guianensis	14	T	28	Nebel 2001
Mouriri	gleasoniana	1	M	12	Flora of Guatemala
Myrcia	splendens	1	U	6	Flora of Peru
Naucleopsis	naga	16	M	15	Gargiullo 2008
Ocotea	bijuga	1	U	10	Gargiullo 2008
Ocotea	floribunda	5	U	10	Gargiullo 2008
Ocotea	hartshorniana	1	U	10	Gargiullo 2008

Ocotea	leucoxylo	1	U	10	Gargiullo 2008
Ocotea	mollifolia	1	U	10	Gargiullo 2008
Pentaclethra	macroloba	111	T	40	World Agroforestry Centre
Perebea	hispidula	1	U	10	Flora of Panama
Peschiera	arborea	1	T	?	Grandtner 2004
Posoqueria	grandiflora	2	U	5	Flora of Costa Rica
Pourouma	bicolor	18	T	35	Sposito and Santos 2001
Pourouma	minor	10	M	18	Mori 1997
Pouteria	durlandii	6	M	12	Flora of Madre de Dios
Pouteria	glomerata	6	T	?	Grandtner 2004
Pouteria	reticulate	6	T	?	Grandtner 2004
Pouteria	Torta	1	T	?	Grandtner 2004
Protium	confusum	7	M	?	Gargiullo 2008
Protium	glabrum	7	M	?	Gargiullo 2008
Protium	panamense	4	M	?	Gargiullo 2008
Protium	pittieri	17	M	15	Gargiullo 2008
Protium	ravenii	9	M	13	Gargiullo 2008
Pseudolmedia	spuria	1	T	30	Herbarium of the Smithsonian Tropical Research Institute
Psychotria	eurycarpa	1	U	5	Flora of Costa Rica
Pterocarpus	rohrii	6	M	13	Lopes et al. 2008
Quiina	macrophylla	1	T	?	Grandtner 2004
Rauvolfia	purpurascens	3	M	?	Grandtner 2004
Rinorea	deflexiflora	11	M	12	Gargiullo 2008
Rollinia	pittieri	1	T	?	Grandtner 2004
Ryania	speciosa	7	M	15	Duke 1993
Sacoglottis	trichogyna	9	T	35	Burger 2005
Saurauia	rubiformis	26	M	15	Hunter 1966
Simarouba	amara	1	T	35	Hardesty 2005
Siparuna	cuspidate	1	M	?	Grandtner 2004
Sloanea	guianensis	1	T	30	Gargiullo 2008
Socratea	exorrhiza	22	P	30	Shumway 2009
Stephanopodium	costaricense	2	M	?	Grandtner 2004
Sterculia	recordiana	3	T	25	Flora of Panama
Swartzia	cubensis	2	T	60	The Wood Explorer Database
Tapirira	guianensis	9	T	30	Janick 2008
Tetragastris	panamensis	5	T	43	O'Brien et al. 1995
Trichilia	septentrionalis	5	T	?	Dominy et al. 2002
Unonopsis	hammelii	3	U	?	Grandtner 2004
Unonopsis	pittieri	6	M	13	Sexton 1964
Virola	koschnyi	7	T	45	Gargiullo 2008
Virola	sebifera	8	T	40	The Wood Explorer Database

Vitex	cooperi	2	T	26	Croat 1978
Vouarana	anomala	1	T	?	Grandtner 2004
Warszewiczia	coccinea	13	M	15	Gargiullo 2008
Welfia	regia	72	P	25	Shumway 2009

8.3 Appendix 3: Species-specific wood densities used to estimate tree biomass.

Genus	Species	Wood density	Source
Anaxagorea	crassipetala	0.65	WAF
Andira	inermis	0.64	Fearnside 1997
Apeiba	membranacea	0.2	Fearnside 1997
Ardisia	fimbrillifera	0.51	WAF
Aspidosperma	spruceanum	0.75	WAF
Balizia	elegans	0.5	Chave 2006
Brosimum	guianensis	0.96	Fearnside 1997
Brosimum	lactescens	0.66	Chave 2006
Brosimum	sp.	0.64	Reyes 1992
Byrsonima	arthropoda	0.64	Reyes 1992
Byrsonima	crispa	0.61	Tropical Timbers of the World
Calophyllum	brasiliense	0.57	Chave 2006
Capparis	pittieri	0.66	Chave 2006
Carapa	guianensis	0.56	Tropical Timbers of the World
Casearia	arborea	0.53	Reyes 1992
Casearia	commersoniana	0.62	Reyes 1992
Casearia	coronata	0.62	Reyes 1992
Casearia	sylvestris	0.71	Chave 2006
Cecropia	insignis	0.32	Chave 2006
Cecropia	obtusifolia	0.31	Chave 2006
Cedrela	odorata	0.43	Chave 2006
Cespedesia	spathulata	0.61	Chave 2006
Chrysophyllum	venezuelanense	0.5	WAF
Cinnamomum	chavarrianum	0.37	WAF
Clarisia	mexicana	0.53	Tropical Timbers of the World
Colubrina	spinosa	0.49	Chave 2006
Conceveiba	pleiostemona	0.27	Chave 2006
Cordia	bicolor	0.43	Reyes 1992
Cordia	dwyeri	0.53	Chave 2006
Cordia	lucidula	0.53	Chave 2006
Croton	schiedeanus	0.484	Chave 2006
Cryosophila	warszewiczii	0.4	Chave 2006
Dendropanax	arboreus	0.42	Chave 2006
Dussia	macrophyllata	0.56	Chave 2006

Erythroxylum	macrophyllum	0.71	Chave 2006
Eschweilera	longirachis	0.85	Fearnside 1997
Eugenia	bacularis	0.765	Chave 2006
Eugenia	sp	0.765	Chave 2006
Ficus	tonduzii	0.32	Reyes 1992
Garcinia	intermedia	0.66	Chave 2006
Goethalsia	meiantha	0.35	Chave 2006
Guarea	bullata	0.44	Fearnside 1997
Guarea	chiricana	0.52	Reyes 1992
Guarea	guidonia	0.68	Fearnside 1997
Guarea	hoffmanniana	0.52	Reyes 1992
Guarea	rhopalocarpa	0.52	Reyes 1992
Guarea	tuerckheimii	0.52	Reyes 1992
Guatteria	aeruginosa	0.36	Reyes 1992
Guatteria	amplifolia	0.51	Chave 2006
Guatteria	diospyroides	0.36	Reyes 1992
Hampea	appendiculata	0.25	Chave 2006
Heisteria	concinna	0.64	Chave 2006
Hernandia	didymantha	0.28	Chave 2006
Hernandia	stenura	0.435	Reyes 1992
Hieronyma	alchorneoides	0.6	Reyes 1992
Hirtella	lemsii	0.795	Chave 2006
Hirtella	media	0.795	Chave 2006
Hymenolobium	mesoamericanum	0.64	Reyes 1992
Ilex	skutchii	0.562	Chave 2006
Inga	acuminata	0.58	Reyes 1992
Inga	alba	0.62	Fearnside 1997
Inga	cocleensis	0.58	Reyes 1992
Inga	densiflora	0.58	Reyes 1992
Inga	leiocalycina	0.56	Chave 2006
Inga	marginata	0.72	Reyes 1992
Inga	pezizifera	0.61	Chave 2006
Inga	ruiziana	0.58	Reyes 1992
Inga	sapindoides	0.58	Reyes 1992
Inga	sertulifera	0.65	Chave 2006
Inga	thibaudiana	0.58	Reyes 1992
Inga	umbellifera	0.72	Chave 2006
Inga	venusta	0.58	Reyes 1992
Jacaranda	copaia	0.35	Chave 2006
Jacaranda	copaia	0.35	Chave 2006
Lacistema	aggregatum	0.5	Chave 2006
Lacmellea	panamensis	0.47	Chave 2006
Laetia	procera	0.65	Chave 2006

Lecythis	ampla	0.75	Chave 2006
Licania	affinis	0.78	Fearnside 1997
Licaria	sarapiquensis	0.82	Fearnside 1997
Maquira	guianensis	0.78	Chave 2006
Marila	laxiflora	0.63	Reyes 1992
Miconia	affinis	0.632	Chave 2006
Miconia	dorsiloba	0.632	Chave 2006
Miconia	elata	0.47	Chave 2006
Miconia	multispicata	0.632	Chave 2006
Miconia	punctata	0.632	Chave 2006
Miconia	sp1	0.632	Chave 2006
Minquartia	guianensis	0.76	Reyes 1992
Mouriri	gleasoniana	0.843	Chave 2006
Myrcia	splendens	0.8	Reyes 1992
Nectandra	cissiflora	0.59	Chave 2006
Ocotea	bijuga	0.51	Reyes 1992
Ocotea	cernua	0.45	Chave 2006
Ocotea	floribunda	0.4	Chave 2006
Ocotea	hartshorniana	0.38	Chave 2006
Ocotea	insularis	0.51	Reyes 1992
Ocotea	laetevirens	0.51	Reyes 1992
Ocotea	leucoxylon	0.45	Reyes 1992
Ocotea	mollifolia	0.51	Reyes 1992
Ocotea	spp.	0.51	Reyes 1992
Ormosia	intermedia	0.59	Fearnside 1997
Pachira	aquatica/acuatika	0.43	Reyes 1992
Pentaclethra	macroloba	0.64	Fearnside 1997
Pleuranthodendron	lindenii	0.68	Chave 2006
Posoqueria	latifolia	0.57	Chave 2006
Pourouma	bicolor	0.36	Chave 2006
Pourouma	minor	0.44	Chave 2006
Pouteria	durlandii	0.69	Chave 2006
Pouteria	glomerata	0.68	Chave 2006
Pouteria	reticulata	0.79	Chave 2006
Pouteria	torta	0.77	Chave 2006
Protium	panamense	0.45	Chave 2006
Protium	pittieri	0.47	Chave 2006
Protium	ravenii	0.65	Fearnside 1997
Pterocarpus	hayesii	0.46	Reyes 1992
Pterocarpus	rohrii	0.41	Reyes 1992
Pterocarpus	sp.	0.46	Reyes 1992
Quararibea	ochrocalyx	0.56	Nogueira et al. 2007
Rauvolfia	purpurascens	0.48	Chave 2006

Rinorea	deflexiflora	0.6	Chave 2006
Rollinia	pittieri	0.27	Chave 2006
Simarouba	amara	0.34	Reyes 1992
Simarouba	amara	0.34	Reyes 1992
Siparuna	cuspidata	0.65	Chave 2006
Sloanea	guianensis	0.82	Chave 2006
Socratea	exorrhiza	0.23	Chave 2006
Sterculia	recordiana	0.49	Chave 2006
Stryphnodendron	microstachyum	0.39	Chave 2006
Swartzia	ochnea	0.95	Reyes 1992
Talisia	nervosa	0.87	Reyes 1992
Tapirira	guianensis	0.5	Fearnside 1997
Tetragastris	panamensis	0.76	Fearnside 1997
Trichilia	septentrionalis	0.656	Chave 2006
Trophis	racemosa	0.66	Chave 2006
Trophis	sp.	0.54	Reyes 1992
Unonopsis	pittieri	0.37	Chave 2006
Virola	koschnyi	0.41	Chave 2006
Virola	sebifera	0.48	Reyes 1992
Vismia	baccifera	0.43	Chave 2006
Vitex	cooperi	0.56	Fearnside 1997
Vochysia	ferruginea	0.4	Chave 2006
Warszewiczia	coccinea	0.56	Chave 2006
Welfia	regia	0.4	Chave 2006
Xylopia	sericophylla	0.54	Chave 2006
Zanthoxylum	panamense	0.49	Chave 2006

9 BIBLIOGRAPHY

- Allen, P. H. 1977. The rain forests of Golfo Dulce. Stanford University Press, Palo Alto, CA.
- Aparicio, A. 2009. Volcán Barva Avian Dataset. Tropical Ecology Assessment & Monitoring Network: DataPackage 20091111162717_2034.
- Aquino, R., T. Pacheco, and M. Vásquez. 2007. Evaluación y valorización económica de la fauna silvestre en el río Algodón, Amazonía peruana. *Revista Peruana de Biología* 14:187-192.
- Armstrong, J. E. and D. Marsh. 1997. Floral Herbivory, Floral Phenology, Visitation Rate, and Fruit Set in *Anaxagorea crassipetala* (Annonaceae), a Lowland Rain Forest Tree of Costa Rica. *Journal of the Torrey Botanical Society* 124:228-235.
- Barlow, J. and C. A. Peres. 2004. Avifaunal responses to single and recurrent wildfires in Amazonian forests. *Ecological Applications* 14:1358-1373.
- Bergen, K. M., A. M. Gilboy, and D. G. Brown. 2007. Multi-dimensional vegetation structure in modeling avian habitat. *Ecological Informatics* 2:9-22.
- Bergen, K. M., R.G. Knox, and Sassan Saatchi, editor. 2006. Multi-dimensional forested ecosystem structure: Requirements for remote sensing observations. NASA Goddard Space Flight Center, Greenbelt, MD.
- Blair, J. B., D.L. Rabine, and M.A. Hofton. 1999. The Laser Vegetation Imaging Sensor (LVIS): A medium-altitude, digitization-only, airborne laser altimeter for mapping vegetation and topography. *ISPRS Journal of Photogrammetry and Remote Sensing* 54:115-122.
- Blair, J. B. and M. A. Hofton. 1999. Modeling laser altimeter return waveforms over complex vegetation using high-resolution elevation data. *Geophys. Res. Lett.* 26:2509-2512.
- Blair, J. B., M.A. Hofton, and D.L. Rabine. 2006. Processing of NASA LVIS elevation and canopy (LGE, LCE and LGW) data products, version 1.01.
- Bongers, F. C.-D., P.; Forget, P.M.; Théry, M., editor. 2001. Nouragues: Dynamics and Plant-Animal Interactions in a Neotropical Rainforest. Springer.
- Botanical Research Institute of Texas (BRIT); Atrium Biodiversity Information System.
- Brokaw, N. V., and R.A. Lent. 1999. Vertical structure. Pages 373-399 in M. Hunter, editor. *Maintaining biodiversity in forest ecosystems*. Cambridge University Press, Cambridge.
- Burger, W. C. H., Michael, editor. 2005. *Flora Costaricensis*. Field Museum of Natural History, Chicago.
- Chambers, J. Q., J. d. Santos, R. J. Ribeiro, and N. Higuchi. 2001. Tree damage, allometric relationships, and above-ground net primary production in central Amazon forest. *Forest Ecology and Management* 152:73-84.
- Chave, J., Muller-Landau, H.C., Baker, T.R., Easdale, T.A., Ter Steege, H. & Webb, C.O. 2006. Regional and phylogenetic variation of wood density across 2456 neotropical tree species. *Ecological Applications* 16:2356-2367.
- Childs, C. 2004. Interpolating surfaces in ArcGIS spatial analyst. *ArcUser* July-September:32-35.

- Choat, B., L. Sack, and N. M. Holbrook. 2007. Diversity of hydraulic traits in nine *Cordia* species growing in tropical forests with contrasting precipitation. *New Phytologist* **175**:686-698.
- Clark, D. B. 2010. Volcán Barva Vegetation Dataset - Trees & Lianas. T. E. A. M. Network DataPackage-20100628103719_4225.
- Clawges, R., K. Vierling, L. Vierling, and E. Rowell. 2008. The use of airborne lidar to assess avian species diversity, density, and occurrence in a pine/aspen forest. *Remote Sensing of Environment* **112**:2064-2073.
- Croat, T. B. 1978. Flora of Barro Colorado Island. Stanford University Press, Palo Alto, CA.
- DeWalt, S. J. and J. Chave. 2004. Structure and Biomass of Four Lowland Neotropical Forests. *Biotropica* **36**:7-19.
- Dominy, N. J., P. W. Lucas, L. W. Ramsden, P. Riba-Hernandez, K. E. Stoner, and I. M. Turner. 2002. Why are young leaves red? *Oikos* **98**:163-176.
- Drake, J. B., R. O. Dubayah, D. B. Clark, R. G. Knox, J. B. Blair, M. A. Hofton, R. L. Chazdon, J. F. Weishampel, and S. Prince. 2002a. Estimation of tropical forest structural characteristics using large-footprint lidar. *Remote Sensing of Environment* **79**:305-319.
- Drake, J. B., R. O. Dubayah, R. G. Knox, D. B. Clark, and J. B. Blair. 2002b. Sensitivity of large-footprint lidar to canopy structure and biomass in a neotropical rainforest. *Remote Sensing of Environment* **81**:378-392.
- Dubayah, R., R. Knox, M. Hofton, J. Blair, & J. Drake. 2000. Land surface characterization using lidar remote sensing. Pages 25-38 in M. H. R. Aspinall, editor. *Spatial Information for Land Use Management* CRC Press, Amsterdam.
- Duke, J. A. D., J. L. 1993. CRC handbook of alternative cash crops. CRC Press, Boca Raton, FL.
- Fearnside, P. M. 1997. Wood density for estimating forest biomass in Brazilian Amazonia. *Forest Ecology and Management* **90**:59-87.
- Fetcher, N., Oberbauer, S. F., and Chazdon, R. L. 1994. Physiological ecology of plants. Pages 128-141 in K. S. B. L. A. McDade, H. A. Hespenheide, and G. S. Hartshorn, editor. *La Selva: Ecology and Natural History of a Neotropical Rain Forest*. University of Chicago Press, Chicago.
- Figuerola-Esquivel, E., F. Puebla-Olivares, H. Godínez-Álvarez, and J. Núñez-Farfán. 2009. Seed dispersal effectiveness by understory birds on *Dendropanax arboreus* in a fragmented landscape. *Biodiversity and Conservation* **18**:3357-3365.
- Finegan, B., M. Camacho, and N. Zamora. 1999. Diameter increment patterns among 106 tree species in a logged and silviculturally treated Costa Rican rain forest. *Forest Ecology and Management* **121**:159-176.
- Flores, E. M. 1992. Trees and Seeds from the Neotropics. Museo Nacional de Costa Rica, San Jose.
- Gargiullo, M. B. 2008. A field guide to plants of Costa Rica. Oxford University Press, Oxford, New York.

- Gerwing, J. J., D. Farias, atilde, and o. Lopes. 2000. Integrating liana abundance and forest stature into an estimate of total aboveground biomass for an eastern Amazonian forest. *Journal of Tropical Ecology* **16**:327-335.
- Glanz, W. E. 1982. The terrestrial mammal fauna of Barro Colorado Island: censuses and long-term changes. in E. G. Leigh, A. S. Rand, and D. M. Windsor, editors. *The ecology of a tropical forest: seasonal rhythms and long-term changes*. Smithsonian Institution Press, Washington, D.C.
- Goetz, S., D. Steinberg, R. Dubayah, and B. Blair. 2007. Laser remote sensing of canopy habitat heterogeneity as a predictor of bird species richness in an eastern temperate forest, USA. *Remote Sensing of Environment* **108**:254-263.
- Goodwin, N. R., N. C. Coops, and D. S. Culvenor. 2006. Assessment of forest structure with airborne LiDAR and the effects of platform altitude. *Remote Sensing of Environment* **103**:140-152.
- Grandtner, M. M. 2004. *World Dictionary of Trees*.
- Hammel, B. E. 1986. New species and notes on *Lauraceae* from the Caribbean lowlands of Costa Rica. *Journal of the Arnold Arboretum* **67**:123-136.
- Harding, D. J., M. A. Lefsky, G. G. Parker, and J. B. Blair. 2001. Laser altimeter canopy height profiles: methods and validation for closed-canopy, broadleaf forests. *Remote Sensing of Environment* **76**:283-297.
- Hernandez, P. A., C. H. Graham, L. L. Master, and D. L. Albert. 2006. The effect of sample size and species characteristics on performance of different species distribution modeling methods. *Ecography* **29**:773-785.
- Hill, R. A., S. A. Hinsley, D. L. A. Gaveau, and P. E. Bellamy. 2004. Cover: Predicting habitat quality for Great Tits (*Parus major*) with airborne laser scanning data. *International Journal of Remote Sensing* **25**:4851-4855.
- Hofton, M. A., L. E. Rocchio, J. B. Blair, and R. Dubayah. 2002. Validation of Vegetation Canopy Lidar sub-canopy topography measurements for a dense tropical forest. *Journal of Geodynamics* **34**:491-502.
- Holdridge, L. R. 2004. *Arboles de Costa Rica*. INBio: the Costa Rican Biodiversity Institute.
- Hunter, G. E. 1966. Revision of Mexican and Central American *Saurauia* (Dilleniaceae). *Annals of the Missouri Botanical Garden* **53**:47-89.
- Janick, J. R. E. P. 2008. *The encyclopedia of fruit & nuts*. CABI, Cambridge, MA.
- Janovec, J. P. and J. S. Harrison. 2002. A Morphological Analysis of the *Compsooneura sprucei* Complex (Myristicaceae), With a New Combination for the Central American Species *Compsooneura mexicana*. *Systematic Botany* **27**:662-673.
- Jullien, M. and J.-M. Thiollay. 1998. Multi-Species Territoriality and Dynamic of Neotropical Forest Understorey Bird Flocks. *Journal of Animal Ecology* **67**:227-252.
- Kapos, V. 1989. Effects of isolation on the water status of forest patches in the Brazilian Amazon. *Journal of Tropical Ecology* **5**:173-185.

- Kearns, T. A. 2005. A methodology for the efficient storage and processing of coastal point data. Pages 2625-2630 Vol. 2623 in *OCEANS*, 2005. Proceedings of MTS/IEEE.
- King, D. A., S. J. Wright, and J. H. Connell. 2006. The contribution of interspecific variation in maximum tree height to tropical and temperate diversity. *Journal of Tropical Ecology* **22**:11-24.
- Laurance, S. G. W. 2004. Responses of Understory Rain Forest Birds to Road Edges in Central Amazonia. *Ecological Applications* **14**:1344-1357.
- Lefsky, M. A., W. B. Cohen, G. G. Parker, and D. J. Harding. 2002. Lidar Remote Sensing for Ecosystem Studies. *BioScience* **52**:19-30.
- Lim, K., P. Treitz, M. Wulder, B. St-Onge, and M. Flood. 2003. LiDAR remote sensing of forest structure. *Progress in Physical Geography* **27**:88-106.
- Lindell, C. A., S. K. Riffell, S. A. Kaiser, A. L. Battin, M. L. Smith, and T. D. Sisk. 2007. Edge responses of tropical and temperate birds. *The Wilson Journal of Ornithology* **119**:205-220.
- Lopes, C., E. Ferraz, and E. d. Araújo. 2008. Physiognomic-structural characterization of dry- and humid-forest fragments (Atlantic Coastal Forest) in Pernambuco State, NE Brazil. *Plant Ecology* **198**:1-18.
- Lugo, A. E. and M. Alayon. 2003. *Big-leaf mahogany: genetics, ecology, and management*. Springer.
- MacArthur, R. H. and H. S. Horn. 1969. Foliage Profile by Vertical Measurements. *Ecology* **50**:802-804.
- MacArthur, R. H. and J. W. MacArthur. 1961. On Bird Species Diversity. *Ecology* **42**:594-598.
- Maltamo, M., P. Packalén, X. Yu, K. Eerikäinen, J. Hyypä, and J. Pitkänen. 2005. Identifying and quantifying structural characteristics of heterogeneous boreal forests using laser scanner data. *Forest Ecology and Management* **216**:41-50.
- Martinuzzi, S., L. A. Vierling, W. A. Gould, M. J. Falkowski, J. S. Evans, A. T. Hudak, and K. T. Vierling. 2009. Mapping snags and understory shrubs for a LiDAR-based assessment of wildlife habitat suitability. *Remote Sensing of Environment* **113**:2533-2546.
- McDade, L. A., Bawa, K. S., Hespeneide, H. A., Hartshorn, G. S. , editor. 1994. *La Selva: ecology and natural history of a neotropical rain forest*. University of Chicago Press, Chicago.
- McShea, W. J. and J. H. Rappole. 2000. *Managing the Abundance and Diversity of Breeding Bird Populations through Manipulation of Deer Populations*
- Manejo de la Abundancia y Diversidad de Aves Reproductoras Mediante la Manipulación de Poblaciones de Venados. *Conservation Biology* **14**:1161-1170.
- Means, J. E., S. A. Acker, D. J. Harding, J. B. Blair, M. A. Lefsky, W. B. Cohen, M. E. Harmon, and W. A. McKee. 1999. Use of Large-Footprint Scanning Airborne Lidar To Estimate Forest Stand Characteristics in the Western Cascades of Oregon. *Remote Sensing of Environment* **67**:298-308.
- Miranda, E. J., N. Priante Filho, P. C. Priante, J. H. Campelo Júnior, G. S. Suli, C. L. Fritzen, J. d. Nogueira, G. L. Vourlitis. . 2004. Maximum leaf photosynthetic light response for three species in a transitional tropical forest in Southern Amazonia. *Revista Brasileira de Engenharia Agrícola e Ambiental* **8**:164-167.

- Mori, S. A. 1997. Guide to the vascular plants of central French Guiana. New York Botanical Garden, New York.
- Nascimento, H. E. M. and W. F. Laurance. 2004. Biomass Dynamics in Amazonian Forest Fragments. *Ecological Applications* **14**:S127-S138.
- Nebel, G. 2001. *Minquartia guianensis* Aubl.: use, ecology and management in forestry and agroforestry. *Forest Ecology and Management* **150**:115-124.
- Nicotra, A. B., R. L. Chazdon, and S. V. B. Iriarte. 1999. Spatial Heterogeneity of Light and Woody Seedling Regeneration in Tropical Wet Forests. *Ecology* **80**:1908-1926.
- Nieder, J. 2001. The flora of the Rio Guajalito mountain rain forest (Ecuador).
- Nogueira, E. M., P. M. Fearnside, B. W. Nelson, and M. B. França. 2007. Wood density in forests of Brazil's 'arc of deforestation': Implications for biomass and flux of carbon from land-use change in Amazonia. *Forest Ecology and Management* **248**:119-135.
- O'Brien, S. T., S. P. Hubbell, P. Spiro, R. Condit, and R. B. Foster. 1995. Diameter, Height, Crown, and Age Relationship in Eight Neotropical Tree Species. *Ecology* **76**:1926-1939.
- Pearman, P. B. 2002. The Scale of Community Structure: Habitat Variation and Avian Guilds in Tropical Forest Understory. *Ecological Monographs* **72**:19-39.
- Pearson, R. G., C. J. Raxworthy, M. Nakamura, and A. Townsend Peterson. 2007. Predicting species distributions from small numbers of occurrence records: a test case using cryptic geckos in Madagascar. *Journal of Biogeography* **34**:102-117.
- Phillips, S. J., R. P. Anderson, and R. E. Schapire. 2006. Maximum entropy modeling of species geographic distributions. *Ecological Modelling* **190**:231-259.
- Puig, C. J. 2005. Carbon sequestration potential of land cover types in the agricultural landscape of eastern Amazonia, Brazil. Cuvillier Verlag.
- Redondo-Brenes, A. V.-A., Braulio; Chazdon, Robin L. 2001. Study of the dynamics and composition of 4 second growth forest in the Huetar Norte region of Costa Rica. . *Revista Forestal Centroamericana* **36**:20-26.
- Reyes, G. 1992. Wood densities of tropical tree species. U.S. Dept. of Agriculture, Forest Service, Southern Forest Experiment Station.
- Roberts, D. L. 2007. Effects of tropical forest fragmentation on ecology and conservation of migrant and resident birds in lowland Costa Rica. University of Idaho, Moscow.
- Rummel, R. J. 1970. Applied Factor Analysis. Northwestern University Press.
- Sarabandi, K. and Y. C. Lin. 2000. Simulation of interferometric SAR response for characterizing the scattering phase center statistics of forest canopies. *Geoscience and Remote Sensing, IEEE Transactions on* **38**:115-125.
- Sawyer, J. O. and A. A. Lindsey. 1971. Vegetation of the life zones in Costa Rica. Indiana Academy of Science.

- Schemske, D. W. and N. Brokaw. 1981. Treefalls and the Distribution of Understory Birds in a Tropical Forest. *Ecology* **62**:938-945.
- Schulenberg, T. S. 1983. Foraging behavior, eco-morphology, and systematics of some antshrikes (Formicariidae: Thamnomanes). *Wilson Bulletin of Ornithology* **95**:505-521.
- Schweinsburg, R. E. 1969. Social behavior of the collared peccary (*Pecari tajacu*) in the Tucson Mountains. Unpubl. Ph.D. dissert., Univ. Arizona, Tucson, 129 pp.
- Şekercioğlu, Ç. H., P. R. Ehrlich, G. C. Daily, D. Aygen, D. Goehring, and R. F. Sandí. 2002. Disappearance of insectivorous birds from tropical forest fragments. *Proceedings of the National Academy of Sciences* **99**:263-267.
- Sexton, O. J., H. Heatwole and D. Knight. . 1964. Correlation of microdistribution of some Panamanian reptiles and amphibians with structural organization of the habitat. *Caribbean Journal of Science* **4**:261-295.
- Shorter, N. S. 2005. Heuristic 3D Reconstruction of Irregularly Spaced Lidar. University of Central Florida, Orlando, FL.
- Shumway, S. W. L., S.L.; Friberg, A.; DeMelo, D. 2009. RainforestPlants.
- Sigel, B. J., W. Douglas Robinson, and T. W. Sherry. 2010. Comparing bird community responses to forest fragmentation in two lowland Central American reserves. *Biological Conservation* **143**:340-350.
- Sigel, B. J., T. W. Sherry, and B. E. Young. 2006. Avian Community Response to Lowland Tropical Rainforest Isolation: 40 Years of Change at La Selva Biological Station, Costa Rica
- Respuesta de la Comunidad Aviar al Aislamiento de Selva Tropical Inundable: 40 Años de Cambios en la Estación Biológica La Selva, Costa Rica. *Conservation Biology* **20**:111-121.
- Skowronski, N., K. Clark, R. Nelson, J. Hom, and M. Patterson. 2007. Remotely sensed measurements of forest structure and fuel loads in the Pinelands of New Jersey. *Remote Sensing of Environment* **108**:123-129.
- Sodhi, N. S., L. H. Liow, and F. A. Bazzaz. 2004. Avian Extinctions from Tropical and Subtropical Forests. *Annual Review of Ecology, Evolution, and Systematics* **35**:323-345.
- Sposito, T. C. and F. A. M. Santos. 2001. Scaling of stem and crown in eight *Cecropia* (Cecropiaceae) species of Brazil. *American Journal of Botany* **88**:939-949.
- Standley, P. 1943. *Studies of Central American Plants III.* .
- Su, J. G. and E. W. Bork. 2007. Characterization of diverse plant communities in Aspen Parkland rangeland using LiDAR data. *Applied Vegetation Science* **10**:407-416.
- Team, R. D. C. 2008. R: A language and environment for statistical computing. *in* R. F. f. S. Computing, editor., Vienna, Austria.
- Terborgh, J., L. Emmons, and C. Freese. 1986. La fauna silvestre de la Amazonía: el despilfarro de un recurso renovable. *Boletín de Lima* **46**:77-85.

- Thiollay, J.-M. 1997. Disturbance, selective logging and bird diversity: a Neotropical forest study. *Biodiversity and Conservation* **6**:1155-1173.
- Toledo, D., L. B. Abbott, and J. E. Herrick. 2008. Cover Pole Design for Easy Transport, Assembly, and Field Use. *Journal of Wildlife Management* **72**:564-567.
- Turner, W., S. Spector, N. Gardiner, M. Fladeland, E. Sterling, and M. Steininger. 2003. Remote sensing for biodiversity science and conservation. *Trends in Ecology & Evolution* **18**:306-314.
- Vierling, K. T., L. A. Vierling, W. A. Gould, S. Martinuzzi, and R. M. Clawges. 2008. Lidar: shedding new light on habitat characterization and modeling. *Frontiers in Ecology and the Environment* **6**:90-98.
- Weishampel, J. F., Ranson, K.J. and Harding, D.J. 1996. Remote sensing of forest canopies. *Selbyana* **17**:6-14.
- Weissenhofer, A. 2005. Structure and vegetation dynamics of four selected one hectare forest plots in the lowland rain forests of the Piedras Blancas National Park ("Regenwald der Österreicher"), Costa Rica, with notes on the vegetation diversity of the Golfo Dulce region. Universität Wien, Wien.
- Willis, E. O. 1972a. The Behavior of Plain-Brown Woodcreepers, *Dendrocincla fuliginosa*. *The Wilson Bulletin* **84**:377-420.
- Willis, E. O. 1972b. The Behavior of Spotted Antbirds. American Ornithologists' Union, Washington.
- World Agroforestry (WAF); Wood Density Database.
- Yi-Cheng, L. and K. Sarabandi. 1999. A Monte Carlo coherent scattering model for forest canopies using fractal-generated trees. *Geoscience and Remote Sensing, IEEE Transactions on* **37**:440-451.